Novel acrylonitrile derived imidazo[4,5-*b*]pyridines as antioxidants and potent antiproliferative agents for pancreatic adenocarcinoma

Ida Boček Pavlinac[1±], Leentje Persoons[2±], Dirk Daelemans[2], Kristina Starčević[3], Robert Vianello[4*] and Marijana Hranjec[1*]

[1]Department of Organic Chemistry, Faculty of Chemical Engineering and Technology, University of Zagreb, Marulićev trg 19, HR-10000 Zagreb, Croatia

[2]KU Leuven Department of Microbiology, Immunology and Transplantation, Laboratory of Virology and Chemotherapy, Rega Institute, Leuven, Belgium

[3]Department of Chemistry and Biochemistry, Faculty of Veterinary Medicine, University of Zagreb, Heinzelova 55, HR-10000 Zagreb, Croatia

[4]Laboratory for the computational design and synthesis of functional materials, Division of Organic Chemistry and Biochemistry, Ruđer Bošković Institute, Bijenička cesta 54, HR-10000 Zagreb, Croatia

± These two authors have contributed equally to this.

* Corresponding authors: Dr. Marijana Hranjec, Full Prof., Department of Organic Chemistry, Faculty of Chemical Engineering and Technology, University of Zagreb, Marulićev trg 20, P.O. Box 177, HR-10000 Zagreb, Croatia, e-mail: mhranjec@fkit.hr; Dr. Robert Vianello, Laboratory for the computational design and synthesis of functional materials, Division of Organic Chemistry and Biochemistry, Ruđer Bošković Institute, Bijenička cesta 54, HR-10000 Zagreb, Croatia, e-mail: robert.vianello@irb.hr

Abstract

We present the design, synthesis, computational analysis, and biological assessment of several acrylonitrile derived imidazo[4,5-*b*]pyridines, which were evaluated for their anticancer and antioxidant properties. Our aim was to explore how the number of hydroxy groups and the nature of nitrogen substituents influence their biological activity.

The prepared derivatives exhibited robust and selective antiproliferative effects against several pancreatic adenocarcinoma cells, most markedly targeting Capan-1 cells (IC_{50} 1.2–5.3 μM), while their selectivity was probed relative to normal PBMC cells. Notably, compound **55**, featuring dihydroxy and bromo substituents, emerged as a promising lead molecule. It displayed the most prominent antiproliferative activity without any adverse impact on the viability of normal cells.

Furthermore, the majority of studied derivatives also exhibited significant antioxidative activity within the FRAP assay, even surpassing the reference molecule BHT. Computational analysis rationalized the results by highlighting the dominance of the electron ionization for the antioxidant features with the trend in the computed ionization energies well matching the observed activities. Still, in trihydroxy derivatives, their ability to release hydrogen atoms and form a stable O–H·····O$^{\bullet}$·····H–O fragment upon the H$^{\bullet}$ abstraction prevails, promoting them as excellent antioxidants in DPPH$^{\bullet}$ assays as well.

Key words: acrylonitriles, antioxidant activity, antiproliferative activity, computational chemistry, imidazo[4,5-*b*]pyridines, pancreatic cancer

1. Introduction

Antioxidants fall into two main categories based on their origin: natural antioxidants, sourced from living organisms, and synthetic derivatives, produced in laboratories or industrial settings.[1] Contrary to popular belief, synthetic antioxidants are often characterized by higher purity and activity compared to their natural counterparts.[2] Both types find utility in various applications such as preserving food and cosmetics, preventing material degradation like rubber, and harnessing their biological properties.[3] These antioxidants come in diverse forms, ranging from enzymes to small organic molecules or trace elements, each varying in size and chemical structure. Current research emphasizes the synthesis and exploration of small molecules that emulate naturally occurring compounds, aiming to uncover novel antioxidants. The antioxidative potential of small molecules typically hinges on four key structural attributes: highly conjugated hydroxyl, amino, thiol, and isoprenoid groups.[4] Among these, antioxidants containing hydroxy groups exhibit diverse complexity, ranging from polyphenols to compounds featuring long alkyl chains such as vitamin E, or simpler conjugated structures like ascorbic acid (AA).[5–7] Additionally, numerous nitrogen-based antioxidants incorporate conjugated active NH groups into their structures.[8]

The effectiveness of polyphenols as antioxidants is linked to both the number and spatial arrangement of hydroxyl groups within a highly conjugated structure.[9,10] Generally, a higher amount of these moieties often corresponds to an increased antioxidative activity, while their further functionalization typically reduces the activity.[11,12] This phenomenon is directly connected to their mode of action. Antioxidants featuring hydroxy groups exert their activity through hydrogen atom transfer (HAT) and single electron transfer (SET) mechanisms, or a combination of both.[13–15] Figure 1 depicts well-known examples of antioxidants containing hydroxy groups.

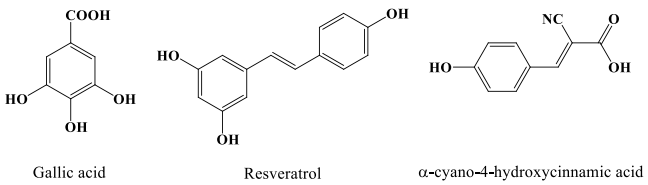

Figure 1. Polyphenolic antioxidants from classes of benzoic acids, stilbenes and cinnamic acids.

Gallic acid, an aromatic carboxylic acid, has garnered extensive attention in research due to its remarkable natural antioxidant properties.[16,17] It is renowned for its capacity to combat oxidative damage and exhibit antiproliferative, antimicrobial, and anti-inflammatory activities.[18–20] Conversely, resveratrol, a derivative of stilbene, is known for its phenolic nature, contributing to its antioxidative capabilities. Its ethene bridge fosters a conjugation between two phenyl rings, enhancing its antioxidative potency through resonance. In constrast, replacing the ethene linker with a single bond or a methylene group significantly diminishes the measured antioxidative activities.[21] This importance of a double bond in driving antioxidative effects is evident in cinnamic acid derivatives. Hydroxy cinnamic acids, prevalent antioxidants in human diets, exhibit notable biological efficacy by potentially thwarting cancer and cardiovascular diseases linked to oxidative-mediated processes.[22,23]

Polyphenols play a protective role against cancer by hindering the cancer cells growth.[24] Although different polyphenols showcase protective properties against cancer, their mechanisms of action vary significantly. The latter encompass antiproliferation, oxidation prevention, anti-inflammatory activity, modulation of cellular signaling, induction of cell cycle arrest or apoptosis, stimulation of detoxification enzymes, estrogenic/antiestrogenic activity, and regulation of the host immune system.[25,26] For instance, research highlights resveratrol's capability to impede all stages of cancer development by suppressing angiogenesis and metastasis. Its anticarcinogenic activity is intricately linked to its antioxidative functions, wherein it inhibits hydroperoxidase, cyclooxygenase, protein kinase C, matrix metalloproteinase-9, and affects the cell cycle.[27] Within our research endeavors, our group focused on investigating the antiproliferative and antioxidative activities of various benzazole compounds possessing critical structural elements crucial for antioxidative efficacy. These elements encompass highly conjugated molecules featuring multiple hydroxyl groups connected by an amide or double bond linker within a benzazole core. Remarkably, the most potent compounds identified featured *N*,*N*-dialkyl chains in the para-position of the phenyl core. These findings validate that promising antioxidants also exhibit substantial inhibitory activity against the pancreatic cancer cell line Capan-1, a cancer type highly sensitive to fluctuations in reactive oxygen species (ROS) concentrations.[28]

In certain cancer types like pancreatic cancer, increased levels of reactive oxygen species (ROS) are observed, contributing to their distinct characteristics marked by high mortality rates and extremely low 5-year survival rates.[29,30] Maintaining a higher concentration of ROS in pancreatic cancer cells over normal cells is essential, striking a delicate balance where it remains elevated enough to affect cancer cells but not excessively

high to induce damage and trigger apoptosis. Considering this scenario, two potential therapeutic strategies emerge: one involves elevating ROS levels to toxic concentrations specifically targeted at pancreatic cancer cells, while the other focuses on limiting ROS production to levels insufficient for cancer development.[31] A combined therapeutic approach could entail the use of chemotherapeutic agents alongside drugs designed to modulate ROS levels. This dual strategy aims to achieve more robust therapeutic outcomes by leveraging the synergistic effects of both approaches.

Many nitrogen heterocycles are considered privileged building blocks in medicinal chemistry and drug design. Due to their properties, they are often introduced to the molecular structure to achieve better solubility, lipophilicity, polarity and hydrogen bonding propensity. Similarity of condensed nitrogen heterocycles with naturally occurring biomacromolecules allows them to form similar interactions with biological systems in cells and express their activity. Considering U.S. FDA approved drugs, five and six membered nitrogen heterocyclic rings are most common, which further emphasizes the importance of studying small molecules like imidazo[4,5-*b*]pyridines in the drug design. [32] Recently discovered imidazo[1,2-*b*]pyridazines substituted with morpholine and indazole inhibited multiple myeloma cell lines MPC-11 and H929 growth. Mechanism of action was proven as the inhibition of transforming growth factor-β activated kinase (TAK1) that is upregulated and overexpressed in multiple myeloma. [33] Another medicinal chemistry breakthrough was achieved by derivatives based on a new class of imidazo[2,1-*b*][1,3,4]thiadiazoles, which not only significantly decreased size of spheroids in MesoII and STO cells, but also inhibited cell migration of the latter by reducing the focal adhesion kinase (FAK) phosphorylation.[34] Furthermore, compounds that share the same heterocyclic core with those successfully inhibiting FAK, showed promising activity against pancreatic adenocarcinoma, namely cell lines SUIT-2, Capan-1 and Panc-1 and gemcitabine-resistant Panc-1R strain. [35] Newly developed 3-amino-1,2,4-triazines revealed a promising anticancer potential targeting pyruvate dehydrogenase kinases (PDK). A combination of *in vitro*, *in silico* and *in vivo* studies suggests that researching small nitrogen heterocycles is a step in the right direction towards obtaining efficient clinical candidates for combatting highly aggressive KRAS-mutant pancreatic ductal adenocarcinoma.[36]

Along these lines, by amalgamating the established antioxidative pharmacophore elements – such as extended conjugation, hydroxy groups, and nitrogen-based heterocycles – we devised novel molecules with potential biological activity based on imidazo[4,5-

b]pyridines. Our study delved into understanding how the number and positioning of hydroxy groups on the phenyl ring affect biological activity. Inspired by the promising inactivation potential of the cyano hydroxy cinnamic acid, we crafted molecules integrating an acrylonitrile group linking the imidazo[4,5-*b*]pyridine core with the phenyl ring. These newly designed compounds underwent testing to assess their antioxidative and antiproliferative activities. Remarkably, in specific cases, bromo-substituted heterocycles displayed elevated antioxidative activity, prompting further exploration into bromo-substituted derivatives. Considering that conjugated NH groups play a pivotal role in numerous antioxidants, we conducted investigations utilizing both N-substituted and N-unsubstituted imidazo[4,5-*b*]pyridines to gain deeper insights into the biological activities associated with this nitrogen-rich heterocyclic core. Selected compounds, exhibiting strong and selective activity against pancreatic cancer cells, were subjected to additional scrutiny to elucidate potential mechanisms of action. Furthermore, computational studies were employed to probe the mechanism of action for compounds demonstrating potent antioxidative activity.

2. Results and Disscussion

2.1. Chemistry

Novel hydroxy and *N*-substituted imidazo[4,5-*b*]pyridine derived acrylonitriles **33-64** were synthesized utilizing established synthetic techniques previously fine-tuned within our research group, following the outlined pathway in Scheme 1. Specifically, **7-9** were produced via an uncatalyzed microwave-assisted amination method, adhering to a procedure published earlier.[28] Compounds **10-12** were synthesized by aminating position 2 on the pyridine ring. The specific conditions for the amination reaction varied based on the presence of a bromo-substituent on the pyridine core. For instances where a bromo-substituent was present, the reaction was conducted in an ice bath. However, in the case of compound **10**, the initial compound **1** was refluxed with an excess of amine. The products from these amination reactions were obtained in moderate to high yields, ranging between 55% and 97%.

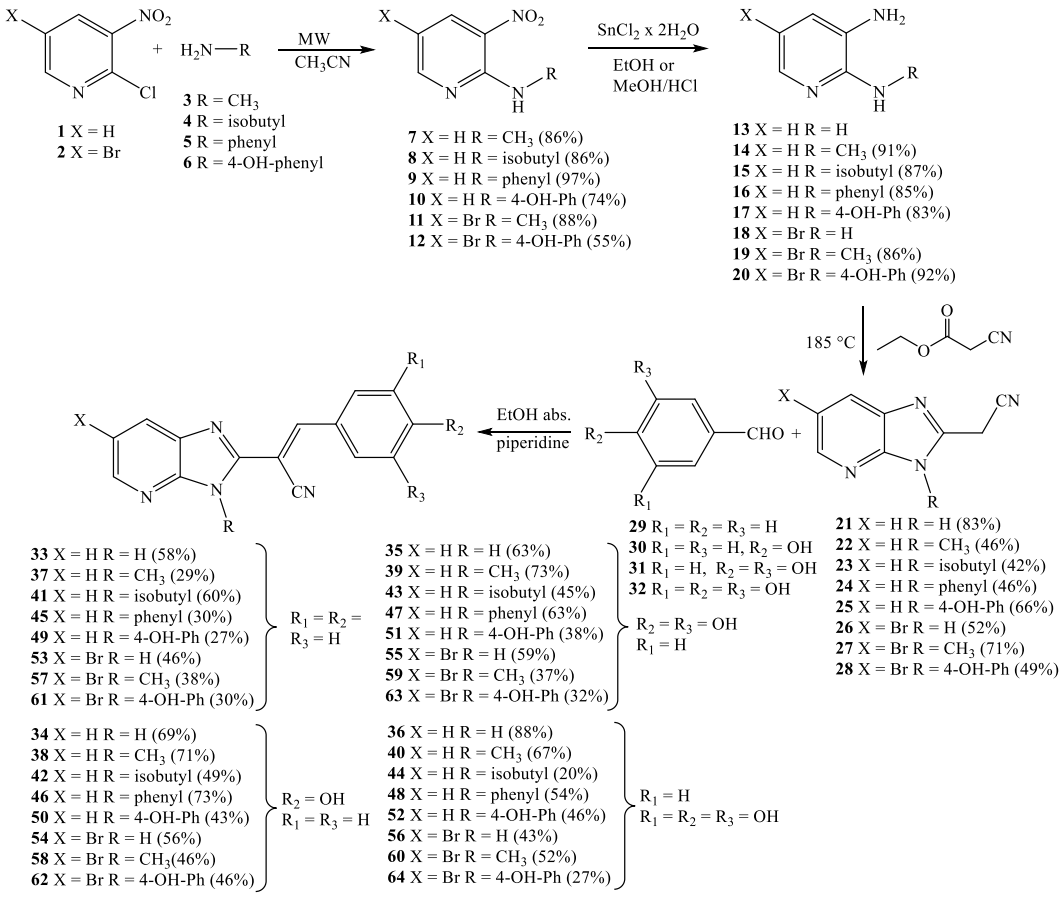

Scheme 1. Synthesis of targeted imidazo[4,5-*b*]pyridine derived acrylonitriles **33-64**

Confirmation of the successful amination was achieved by analysing the ^{1}H NMR spectra, demonstrating the appearance of NH proton signals along with the corresponding signals related to the amino chain or ring. In cases involving aromatic amines, the NH protons experienced deshielding, leading to signals detected in the range from 9.96–9.36 ppm. Meanwhile, NH protons shielded by aliphatic groups displayed signals within the range of 8.54–8.47 ppm. Additionally, the presence of additional carbon atoms attached to the amino group was observed in the ^{13}C spectrum. Subsequent reduction of the nitro group to amino using $SnCl_2 \times 2H_2O$ resulted in the isolation of 2,3-diaminopyridines **13-20** in very favorable yields (ranging from 80% to 92%). Notably, this reduction significantly influenced the position of NH protons in the ^{1}H NMR spectra, causing a shift of signals upfield. This shift ranged from 5.82-5.47 ppm for aliphatic compounds and 7.70-7.40 ppm for aromatic amines. A new signal corresponding to the protons of the amino group appeared in the range of 5.31–4.59 ppm.

Table 1. Chemical shifts of specific protons of acrylonitrile derivatives in ^{1}H NMR spectrum

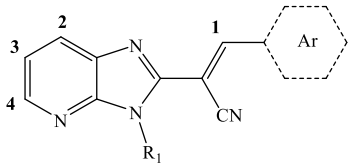

CPD	H-1	H-2	H-3	H-4
33	8.40	8.09	7.31	8.41
34	8.30	8.03	7.27	8.37
35	8.20	8.02	7.27	8.36
36	8.10	8.01	7.26	8.35
37	8.31	8.16	7.38	8.46
38	8.15	8.11	7.35	8.42
39	8.05	8.11	7.35	8.42
40	7.93	8.10	7.35	8.41
41	7.94	8.27	7.45	8.39
42	7.82	8.22	7.41	8.36
43	7.67	8.20	7.41	8.34
44	7.48	8.17	7.39	8.31
45	8.41	8.18	7.39	8.46
46	8.25	8.12	7.36	8.42
47	8.13	8.12	7.35	8.41
48	7.89	7.98	7.25	8.28
49	8.43	8.23	7.42	8.38
50	7.77	8.14	7.36	8.29
51	7.56	8.07	7.32	8.23
52	7.42	8.03	7.28	8.20
53	8.37	8.46	/	8.49
54	8.30	8.31	/	8.44
55	8.22	8.29	/	8.44
56	8.12	8.28	/	8.43
57	8.33	8.46	/	8.55
58	8.17	8.40	/	8.51
59	8.06	8.39	/	8.50
60	7.81	8.21	/	8.35
61	8.01	8.47	/	8.57
62	7.56	8.27	/	8.30
63	7.80	8.37	/	8.42
64	7.41	8.22	/	8.24

The imidazo[4,5-*b*]pyridine core was obtained via the cyclocondensation reaction of 2,3-diaminopyridines **13-20** using ethyl-cyanoacetate. Despite the isolation of cyanomethyl derivatives **21-28** in good yields (ranging from 46% to 83%), steric hindrance from phenyl and isobutyl substituents was evident. In the ^{1}H NMR spectra of these compounds, a singlet for the methylene group was observed. The appearance of this singlet, shifting upfield

compared to the signal of the amino group, and the disappearance of the signal for the NH proton confirmed the successful cyclization. To investigate the influence of the number and position of hydroxyl groups on biological activity, we synthesized targeted compounds **33-64** through the reaction between cyanomethyl derivatives of imidazo[4,5-*b*]pyridine **21-28** and benzaldehydes **29-32**. The yields of these products varied widely, ranging from 20% to 83%, which was notably dependent on the compounds' crystallization ability. The purification of hydroxy-substituted acrylonitriles posed challenges as they strongly interacted with silica gel, preventing purification using normal phase column chromatography. Compounds **49-53** and **61-64**, bearing 4-hydroxyphenyl substituents at the N3 position, exhibited lower overall yields, suggesting potential steric hindrance due to the aldol condensation. Furthermore, 6-bromo-substituted **53-64** were isolated in lower overall yields compared to their unsubstituted counterparts. Table 1 provides a detailed analysis of CH and pyridine protons of the targeted compounds. The signals of pyridine core protons in 6-bromo-substituted derivatives were detected in lower magnetic fields due to the presence of electronegative bromo atoms causing deshielding. However, this did not significantly impact the signal of the acrylonitrile group.

The position of pyridine protons in the ^{1}H NMR spectrum was notably influenced by both the imidazo[4,5-*b*]pyridine N3-substituents and the number of phenyl hydroxyl groups. Pyridine protons exhibited increased shielding with a higher number of hydroxyl groups. The chemical shifts in ^{1}H NMR spectrum of some specific protons are shown in the Table 1.

2. Biological activity

2.1. Antitumor activity

The targeted compounds were tested against several cancer cell lines to evaluate their *in vitro* antiproliferative activity. For this, four diverse solid tumor cancer cell lines were chosen, i.e. LN-229 (glioblastoma), Capan-1 (pancreatic adenocarcinoma), HCT-116 (colorectal carcinoma), and NCI-H460 (lung carcinoma). In addition, four hematological cancer cell lines were selected, namely DND-41 (acute lymphoblastic leukemia), HL-60 (acute myeloid leukemia), K-562 (chronic myeloid leukemia), and Z-138 (non-Hodgkin lymphoma). The results for compounds displaying IC_{50} values below 50 µM are summarized as a heatmap in Figure 2, panel A, and standard antitumor drug etoposide (ETO) is included as a reference control. An overview of the complete table of results can be found in supplementary Table 1. The obtained results indicate that the antiproliferative efficacy of the

tested compounds is highly dependent on the number of hydroxy groups present. The majority of the tested compounds demonstrated moderate activity, while certain compounds exhibited pronounced antiproliferative activity, and this was mainly observed against the pancreatic adenocarcinoma cell line Capan-1. For this cell line, the most promising and potent derivative is the bromo-substituted derivative **56** bearing three hydroxy groups, demonstrating robust and selective activity specifically against Capan-1 cells (1.9 μM). The same selectivity towards pancreatic adenocarcinoma (IC_{50} value of 3.0 μM against Capan-1) was noted for **43**, bearing two hydroxy groups at positions 3 and 4 of the phenyl ring, with the phenyl ring positioned at the N3 atom of imidazo[4,5-*b*]pyridine. When comparing **56**, with three hydroxy groups, and **63**, with four such moieties, it can be inferred that the additional hydroxy group leads to a reduction in antiproliferative activity against Capan-1 cells. Also, the bromo-substituted compound **60**, with a methyl group positioned at the imidazo[4,5-*b*]pyridine N-atom, demonstrated similar selectivity towards Capan-1 cells with an IC_{50} value of 3.2 μM. Furthermore, the bromo-substituted derivative **55**, bearing two hydroxy groups, also displayed a potent activity against Capan-1 cells (2.1 μM), however, this activity was expanded to encompass broad antitumoral efficacy across multiple cancer cell lines. A similar broad antitumoral activity pattern was noted for the bromo-substituted **54**, bearing one hydroxy group.

The majority of compounds exhibited notable and selective activity primarily against the Capan-1 cancer cell line (1.9–12.8 μM), albeit with lower activity compared to the included reference drug etoposide. In general, the substitution of pyridine with bromine was observed to enhance the antiproliferative activity of all bromo-substituted acrylonitrile derivatives. The most active compounds were unsubstituted at the N-atom of the imidazo[4,5-*b*]pyridine nuclei. To ascertain whether the observed antiproliferative activity is selective towards cancer cells, the cytotoxicity against normal peripheral blood mononuclear cells (PBMC) were assessed (Figure 2B). No negative effect on the viability of PBMC was observed, as evidenced by IC_{50} values consistently exceeding 50 μM, indicating promising anticancer selectivity.

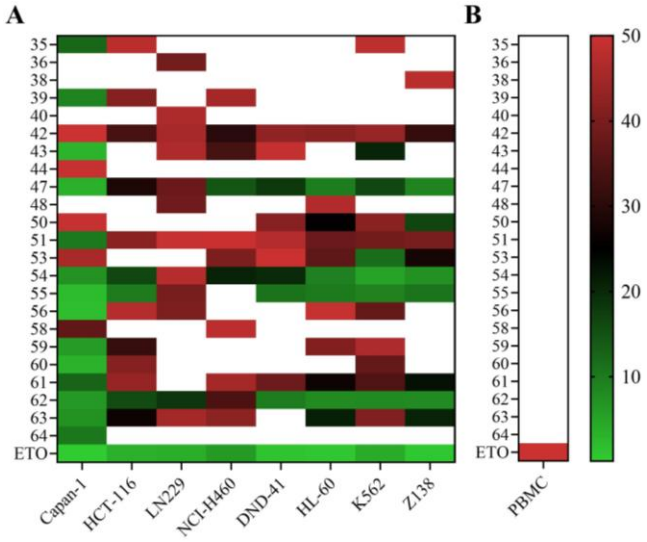

Figure 2. Heatmap depicting the cell growth inhibition induced by derivatives **33**–**64**. (A) Results in a panel of diverse cancer cell types, (B) the effects on normal peripheral blood mononuclear cells (PBMC). Cellular responses were visualized as a heatmap, with IC_{50} values (µM) plotted for each compound. Light green signifies robust inhibition of cell growth (low IC_{50} values), while red indicates minimal to no impact on cell viability (high IC_{50} values). White represents IC50 values above 50 µM.

Since a general selectivity towards the pancreatic adenocarcinoma cell line Capan-1 was observed for several derivatives, two additional pancreatic adenocarcinoma cell lines (MIA PaCa-2 and PANC-1) were included to investigate the potential tissue-specific nature of this phenomenon (Figure 3A). The findings revealed that Capan-1 exhibited the highest sensitivity to inhibition by the series of acrylonitriles, and a similar broad antitumoral activity pattern was noted across the two additional pancreatic cell lines, pointing towards a cell line specific rather than a tissue type specific effect. The complete table of results for the two additional pancreatic adenocarcinoma cell lines can be found in supplementary Table 2.

Next, we focused on examining the impact of a selection of three potent derivatives, namely **47**, **54** and **55**, on the growth of Capan-1 pancreatic adenocarcinoma cells within a three-dimensional (3D) culture. This approach is considered a more representative model for *in vitro* drug testing, as it mirrors various *in vivo* characteristics of tumors. Exposure of 3D spheroid cultures to these three acrylonitrile derivatives induced visible alterations in the morphology and size of the obtained spheroids of the investigated cell line (Figure 3B). The selected derivatives consistently exhibited dose-dependent inhibition of Capan-1 spheroid growth, with corresponding IC_{50} values illustrated in Figure 3C.

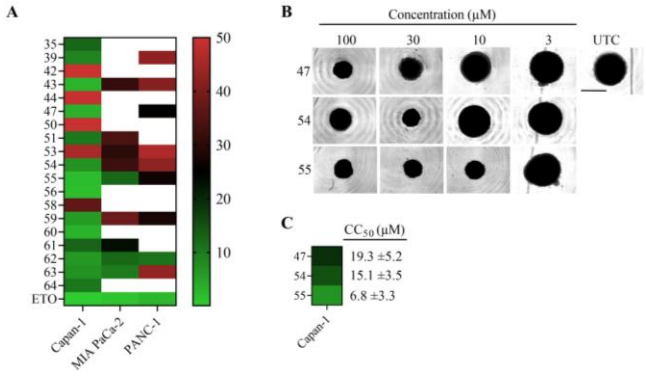

Figure 3. Heatmap illustrates the inhibition of cell growth caused by the indicated hydroxyl and *N*-substituted imidazo[4,5-*b*]pyridine derived acrylonitriles **33**-**64**. (A) results in three pancreatic adenocarcinoma cell lines. (B) the growth of Capan-1 tumor spheroids was dose dependently prevented by the addition of derivatives **47**, **54** and **55**, and corresponding CC_{50} values are depicted in (C). UTC, untreated control. Scale bars, 700 µm.

In order to further characterize the most potent derivatives as novel inhibitors of Capan-1 pancreatic adenocarcinoma cells, we investigated the effect of these compounds on the cell cycle distribution of Capan-1 cells. DAPI staining was conducted to assess the cell cycle progression following treatment with various doses of compounds **47**, **54** and **55**. The findings indicate that exposure of Capan-1 cells to the compounds did not significantly alter the cell cycle distribution, at either tested concentration (Figure 4).

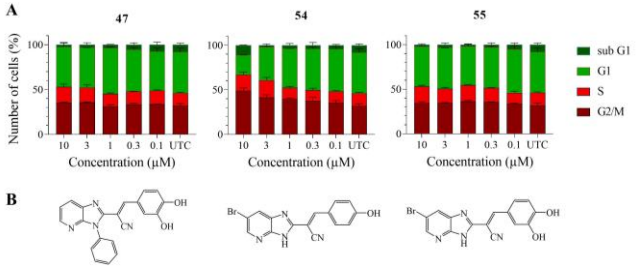

Figure 4. Effect on cell cycle distribution in Capan-1 cells. (A) Capan-1 cells were treated with indicated concentrations of **47**, **54** and **55** for a duration of 24 hours. Following DAPI staining, the distribution of cell cycle was evaluated through high content analysis, and the proportion of cells in each phase was quantified. (B) Corresponding chemical structures of lead compounds **47**, **54** and **55**.

Table 2. Antioxidative activity *in vitro*

CPD	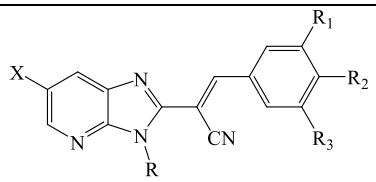					FRAP mmolFe^{2+}/mmolC	ABTS/µM	DPPH/µM
	R	**X**	**R_1**	**R_2**	**R_3**			
33	H	H	H	H	H	45.4±0.6	2220±110	236.9±1.4
34	H	H	H	OH	H	83.7±2.2	2990±130	151.1±1.6
35	H	H	H	OH	OH	5366.4±206.2	16.7±0.6	1.398±0.5
36	H	H	OH	OH	OH	4725.0±187.9	12.9±0.8	$2.0\pm8.9\times10^{-5}$
37	methyl	H	H	H	H	17.9±0.6	-*	652.9±12.3
38	methyl	H	H	OH	H	22.4±3.1	880.6±120	49.9±6.5
39	methyl	H	H	OH	OH	4473.2±167.9	20.9±3.3	3.8±1.4
40	methyl	H	OH	OH	OH	3967.2±30.8	15.5±5.7	0.8±0.0
41	isobutyl	H	H	H	H	663.6±15.8	-	-
42	isobutyl	H	H	OH	H	34.18±1.51	-*	200±5.7
43	isobutyl	H	H	OH	OH	3628.8±5.0	36.8 ± 2.6	1.2 ±0.0
44	isobutyl	H	OH	OH	OH	1911.4±40.3	90.4 ±7.4	1.9± 0.1
45	phenyl	H	H	H	H	1124.5±22.2	-	-
46	phenyl	H	H	OH	H	19.93±0.50	-*	110±20
47	phenyl	H	H	OH	OH	3329.5±55.4	51.8 ±7.6	1.5±0.1
48	phenyl	H	OH	OH	OH	2893.0±68.0	67.4 ±1.7	1.7 ± 0.0
49	4-OHphenyl	H	H	H	H	1076.0±16.6	5460±46.7	13.5 ±1.9
50	4-OHphenyl	H	H	OH	H	86.3±0.7	883±120	81.1±5.9
51	4-OHphenyl	H	H	OH	OH	2854.4±24.7	23.5±0.6	1.9±0.3
52	4-OHphenyl	H	OH	OH	OH	2153.7±45.3	104±7.0	0.4 ±0.0
53	H	Br	H	H	H	315.5±14.9	-	18.3±0.4
54	H	Br	H	OH	H	64.9±6.1	106.4±7.07	23.0±3.2
55	H	Br	H	OH	OH	4594.3±67.2	100.0±26	3.7±0.4
56	H	Br	OH	OH	OH	4166.8±27.6	70.8±2.4	3.7±1.2
57	methyl	Br	H	H	H	75.7±1.9	828.4±20	3650±0.0
58	methyl	Br	H	OH	H	21.0±0.4	1756±700	363.9±24.3
59	methyl	Br	H	OH	OH	4223.8±18.2	153.4±30	9.0±0.9
60	methyl	Br	OH	OH	OH	2597.9±17.8	33.2±0.9	11.3±0.2
61	4-OHphenyl	Br	H	H	H	58.4±2.1	401.4±20	1341.5±23.3
62	4-OHphenyl	Br	H	OH	H	155.4±1.7	101.3±0.7	101.3±23.3
63	4-OHphenyl	Br	H	OH	OH	2127.5±32.2	31.6±0.4	1.0±0.3
63	4-OHphenyl	Br	OH	OH	OH	1374.6±6.5	54.3±1.9	1.5±0.3
BHT	-	-	-	-	-	2089.3±55.9	23.12±1.2	25±4.2

* No activity was observed.

2.2. Antioxidative activity *in vitro*

The *in vitro* antioxidative activity of the prepared acrylonitriles was assessed with three methods, namely DPPH, ABTS and FRAP assays. Data in Table 2 indicate that certain compounds exhibited greater antioxidative potential than butylated hydroxytoluene (BHT), which was used as a standard. Particularly noteworthy was the pronounced antioxidative activity in compounds featuring two or three hydroxyl groups on the phenyl ring. Furthermore, in the FRAP assay, the substituent positioned at the N3 of the imidazo[4,5-*b*]pyridine core significantly influenced the antioxidative activity, with either no substituent or small alkyls such as the methyl group proving optimal at that specific site. Bromo-substituted compounds demonstrated less activity relative to their unsubstituted counterparts. The antioxidative activity was notably impacted by the number of hydroxyl groups, with the most active compounds in the FRAP assay containing two or three such moieties. Compound **35**, without a substituent at the N3 position of the imidazo[4,5-*b*]pyridine core and two hydroxyl groups on the phenyl ring, showed the highest antioxidative activity (5366,4 mmolFe^{2+}/mmolC). In DPPH and ABTS radical scavenging assays, the number of hydroxyl groups played a significant role in achieving antioxidative potential. Bromo-substituted derivatives displayed less antioxidative potential relative to unsubstituted analogues. The most pronounced activities were observed for compounds bearing three hydroxyl groups, such as **40** (DPPH IC_{50} 0.785 μM, ABTS: 15.55 μM) and the 3,4-dihydroxy substituted **36** (DPPH: IC_{50} 2.093 μM, ABTS: 12.99 μM). In the DPPH assay, **52** featuring four hydroxyls, showed a prominent antioxidative activity (DPPH: IC_{50} 0.44 μM). Generally, most compounds demonstrated a higher potential for reducing DPPH radical relative to ABTS.

2.3. Hemolysis protective effect

The hemolysis of erythrocytes induced by hydrogen peroxide (H_2O_2) is a widely employed biological model to assess antioxidant activity. In order to explore the potential association between the *in vitro* antioxidative and antiproliferative effects, all derivatives were evaluated through a red blood cell hemolytic assay. L-ascorbic acid (L-AA) served as the positive control, while phosphate buffer (PBS) was included as the negative control. Following the addition of hydrogen peroxide, inducing lipid peroxidation of the erythrocyte membrane, spectrophotometric measurements were employed to quantify the extent of hemolysis. The results were compared to the included control samples (PBS), in which maximal hemolysis occurs (defined as 100% hemolysis). In the majority of derivatives, a

protective effect was observed in a dose-dependent manner. In Figure 5A, the heatmap depicts the results for compounds that inhibited the hemolysis of red blood cells with at least 50%. The results indicate that elevating the concentration of the compound correlates with an increased protective effect against erythrocyte hemolysis.

The Pearson correlation coefficient (PCC) was determined to evaluate the strength and direction between the three biological activity datasets: cancer cell proliferation, antioxidative activity measured by FRAP analysis, and erythrocyte hemolysis. The correlation was computed pairwise between each dataset. The IC_{50} values in Capan-1 served as a first dataset, FRAP antioxidative activity was included as a second set, and lastly the IC_{50} values obtained from the hemolysis assay in erythrocytes was added as a third parameter. A heatmap representing the correlation matrix was generated (Figure 5B).

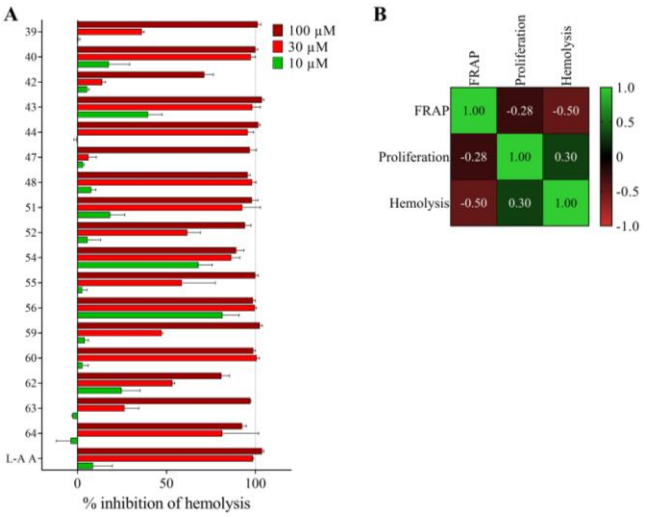

Figure 6. Protective effects of imidazo[4,5-*b*]pyridines on H_2O_2-induced erythrocyte hemolysis assay. (A) Erythrocytes were pretreated with different concentrations (100 - 30 - 10 µM) of the test compounds for 15 minutes prior to H_2O_2 treatment for 2 hours. The relative hemolysis was assessed in comparison with the hemolysis in the H_2O_2 treated negative control (PBS), which was set as 100 %. (B) Heatmap representation of the correlation between the three biological activity datasets (proliferation, hemolysis and FRAP).

A low positive correlation (r = 0.30) was identified between the IC_{50} values from the proliferation and hemolysis experiments. With the addition of the FRAP dataset, an expected negative correlation was anticipated due to the inverse relationship between high FRAP assay values and IC_{50} data. As such, a moderately negative correlation was observed between FRAP

and the hemolysis assay (r = –0.50). Lastly, negligible correlation was found between FRAP and the IC_{50} values in Capan-1. Therefore, the antioxidative activities of the synthesized acrylonitrile derivatives, whether assessed through FRAP or the hemolysis assay, seem to be unrelated to their antiproliferative activities. Future experiments are necessary to unravel the underlying mechanism of action for these compounds concerning their anticancer effects.

2.4. Computational analysis

Computational analysis was employed to provide additional insights into the structure and properties of the studied systems, aiming to elucidate the pertinent processes contributing to their antioxidant characteristics. Due to the substantial number of structurally similar systems under examination here, a focused selection of derivatives was chosen for in-depth analysis, specifically encompassing compounds **33–36**, **40**, **48**, **52** and **56**. This approach enables an examination of the impact of multiple hydroxyl groups on the radical scavenging ability of the synthesized conjugates. Additionally, it allows for an exploration of the influence of further alkyl and aryl substitutions on the imidazo[4,5-*b*]pyridine moiety of the studied derivatives. The obtained results will be discussed relative to the standard system BHT. The data presented in Table 6 shows the single-electron ionization energy (IE) and electron affinity (EA) of each derivative, along with the bond dissociation energy (BDE), indicating its capacity for thermodynamically favorable homolytic cleavage of the hydrogen atom ($H^{\bullet}$). To appropriately contextualize these values, they should be evaluated in conjunction with the corresponding data for the reference systems employed in each assay, specifically $ABTS^{\bullet+}$, $DPPH^{\bullet}$ and FRAP (Table 6).

Table 6. The ionization energies (IEs), electron affinities (EAs), and homolytic X–H bond dissociation energies (BDEs) or bond association energies (BAEs) are reported for the ethanol solution. All values are expressed in kilocalories per mole (kcal mol^{-1}) and are calculated using the (SMD)/B3LYP/6–31+G(d) model.

System	Structure	IE	EA	BDE/BAE	Site
33	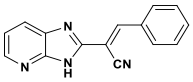	135.6	71.2	85.8	N–H
34	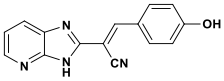	130.4	69.9	70.9	*p*-O–H
35	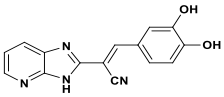	128.4	69.9	65.0	*p*-O–H
36	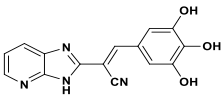	129.2	70.5	61.3	*p*-O–H
40	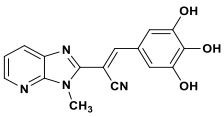	130.5	68.1	63.0	*p*-O–H
48	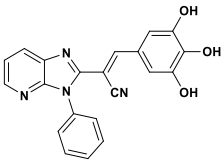	130.1	68.8	62.2	*p*-O–H
52	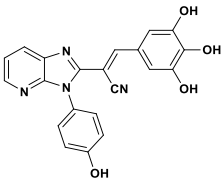	129.7	68.7	62.0	*p*-O–H
56	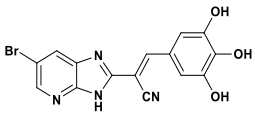	130.4	71.7	61.8	*p*-O–H
BHT	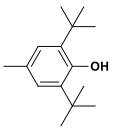	125.3	18.7	62.0	O–H
FRAP	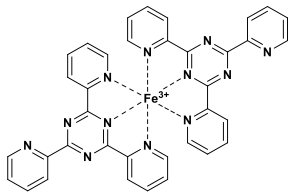		147.0		
ABTS$^{\bullet+}$	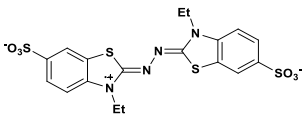	111.2	125.3	–36.6	N$^{\bullet+}$
DPPH$^{\bullet}$	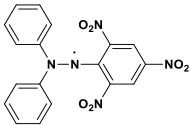	104.5	124.5	–66.6	N$^{\bullet}$

The FRAP assay represents a straightforward system in which its radical scavenging ability predominantly relies on the electron-accepting mechanism that reduces a ferric Fe(III) complex into its ferrous Fe(II) analogue. According to both literature and our data, FRAP is an excellent radical scavenger, as evidenced by a high electron affinity (EA) of 147.0 kcal mol^{-1}. This EA surpasses the ionization energies of all our systems (Table 6), thereby supporting the thermodynamic feasibility of the electron-transfer process. The situation is less straightforward for the other two assays, $ABTS^{\bullet+}$ and $DPPH^{\bullet}$, since their EA values cluster around 125 kcal mol^{-1}, which leaves only a modest feasibility to exchange electrons with the synthesized compounds. However, all systems possess ionization energy (IE) values that extend up to 135 kcal mol^{-1}, allowing certain feasibility for the Single Electron Transfer (SET) mechanism even in these two assays. When considering the exergonicity of the hydrogen atom transfer onto $ABTS^{\bullet+}$ (–36.6 kcal mol^{-1}) and $DPPH^{\bullet}$ (–66.7 kcal mol^{-1}) and noting that all computed hydrogen atom abstraction energies for our systems cluster between 60–70 kcal mol^{-1}, it indicates that the Hydrogen Atom Transfer (HAT) mechanism is highly unlikely with $ABTS^{\bullet+}$, yet moderately feasible with $DPPH^{\bullet}$. Therefore, we can conclude that the SET mechanism likely predominates in determining the antioxidant capacity of our compounds in all three assays, with some relevance of the HAT mechanism for the $DPPH^{\bullet}$ assay. This context will guide our interpretation of the observed trends in the measured activites.

We intiate the analysis with the unsubstituted parent compound **33**. Its IE, EA and BDE values are the most endergonic among the studied systems, affirming its poor antioxidant properties in all three examined assays. The introduction of the electron-donating –OH group in **34** enhances its ability to both donate and accept an electron, resulting in improvements in across assay parameters. In addition, while the $H^{\bullet}$ release in **33** relied on the abstraction from the imidazole N–H moiety with a BDE of 85.8 kcal mol^{-1}, the introduced –OH group in **34** allows a significantly more feasible $H^{\bullet}$ abstraction at a BDE of 70.9 kcal mol^{-1}, which largely surpasses both improvements brought to IE and EA values, which are within the range of 1–5 kcal mol^{-1}. Still, such a large reduction in BDE of around 15 kcal mol^{-1} remains unevident in the measured assays, since the energy required for $DPPH^{\bullet}$ to accept $H^{\bullet}$ in only –66.7 kcal mol^{-1}, thus still leaving a thermodynamical mismatch of around 4 kcal mol^{-1} among values. Therefore, even in the $DPPH^{\bullet}$ assay, the antioxidant activity of **34** predominantly relies on the electron transfer reaction, leading to a much smaller, only around 1,5-fold improvement in $DPPH^{\bullet}$ data.

The second electron-donating –OH group in **35** further enriches the system with electronic density, which allows an additional reduction in its IE value, seen as a large increase in FRAP activity. It also reduces the BDE to 65.1 kcal mol^{-1}, thus being below the exergonicity of attaching H$^{\bullet}$ to DPPH$^{\bullet}$. This reduction likely accounts for the over 10-fold increase observed in the DPPH$^{\bullet}$ activity. Interestingly, due of steric crowding from three vicinal –OH groups, the third hydroxyl moiety in **36** hinders their ability to donate electrons to the rest of the system, also partly residing in their electronic density investment for the formation of two O–H·····O hydrogen bonds in the initial system. This results in an increase in its IE value from 128.4^{-1} in **35** to 129.2 kcal mol^{-1} in **36**. This is seen in lower FRAP and unchanged ABTS parameters in **36** relatives to **35**. However, the adjacent three –OH groups in **36** allow for a very efficient hydrogen atom abstraction from the middle *para*-OH group. This process forms a very stable and resonantly stabilized O–H·····O$^{\bullet}$·····H–O fragment with a remarkably low BDE of 61.3 kcal mol^{-1}, even surpassing the reference BHT (BDE = 62.0 kcal mol^{-1}). This confirms its exceptional activity in the DPPH assay of 2·10^{-5} μM, being by far the most potent antioxidant among those measured in that assay. This leads us to conclude that the 2,3,4-trihidroxy unit represents the best compromise between the electron-donating and hydrogen atom releasing capabilities of neighboring hydroxy groups, affording pronounced antioxidant activites in all three assays. It is noteworthy to mention that if a system with an excessive ability to release electrons and highly favorable FRAP parameters is desired, a dihydroxy system likely provides the most efficient solution.

With this in mind, the rest of our analysis maintains the 2,3,4-trihidroxy fragment and evaluates the effect of various substituents on the imidazo[4,5-*b*]pyridine core, with reference to system **36**. Bromination of the pyridine unit has very little effect on the calculated parameters, yet consistently making IE, EA and BDE values more endergonic and the underlying processes more difficult to achieve. This stems from 0.5 kcal mol^{-1} in BDE to 1.2 kcal mol^{-1} in both IE and EA parameters. Consequently, practically all Br-containing derivatives are measured as less potent antioxidants than their unsubstituted analogs, which confirms experimental observations. On the other hand, the imidazole nitrogen represents a very convenient site to introduce various alkyl and aryl substituents with the idea to fine tune the antioxidant activites. Yet, our analysis reveals only a marginal effect when substituents are introduced at this site. This is evident in the narrow ranges of 1.3, 2.4 and 1.7 kcal mol^{-1} seen for all IE, EA and BDE values in systems **36**, **40**, **48** and **52** respectively. Consequently, no consistent conclusions can be drawn on the impact of these substitutions.

It is noteworthy that aryl groups are somewhat more favorable for relevant IE and BDE values over their alkyl analogues, yet even in those cases the computed values indicate more endergonic processes than in the unsubstituted **36**. As such, the precise order of antioxidant activities strongly depends on the design of the rest of the molecular system, as seen in the range of activities observed here, with a variable conclusion that unsubstituted imidazole units usually provide more potent antioxidants. As an illustrative example, when the parent unsubstituted conjugate **33** is considered, its *N*-phenyl (**45**) and, especially, *N*-4-hydroxyphenyl (**49**) derivatives offer stronger antioxidants based on the electron-donating effect of both aromatic substituents and the $H^{\bullet}$ donating ability of the latter. Still, with the introduction of the first -OH group to **33**, the system **34** surpasses the antioxidant potency of both of its *N*-phenyl (**46**) and *N*-4-hydroxyphenyl (**50**) derivatives, the latter consistently being the case in other di- and tri-hidroxy analogues as well.

Lastly, we note that bromine incorporation reduces antioxidative activity (see Table 6 for **36** and **56**) by increasing the ionization energy by 1.2 kcal mol^{-1}, which translates to around 8 times lower antioxidant potency. Yet, at the same time, it was demonstrated here that such a substitution improves the antiproliferative properties, which could be taken as an indirect proof that antioxidant features of investigated systems are not predominantly responsible for their antiproliferative activities, which confirms experimental observations reported here.

3. Conclusion

This study outlines the development, synthesis, computational analysis, and biological evaluation of novel hydroxy and N-substituted imidazo[4,5-b]pyridine derived acrylonitriles. The design of these targeted acrylonitriles aimed to scrutinize the influence of both the number of hydroxyl groups and the nature of the substituent attached to the N atom of imidazo[4,5-*b*]pyridine on their biological activities. All compounds were synthesized using established organic synthesis methods refined within our research group.

In vitro testing of the synthesized compounds was conducted to assess their antiproliferative activity against specific cancer cell lines. The findings unveiled notable and selective antiproliferative effects, particularly against pancreatic adenocarcinoma cells. Certain compounds exhibited impressive IC_{50} values ranging from 1.9 to 3.0 μM. Following this, promising compounds underwent further testing against additional pancreatic

adenocarcinoma cell types in both 2D and 3D systems, alongside normal peripheral blood mononuclear cells (PBMC). Compound **55**, which featured bromo-substitution and two hydroxy groups, displayed robust antiproliferative activity against Capan-1 cells. Generally, it was observed that substituting pyridine nuclei with bromine and the presence of an NH group on the imidazo[4,5-*b*]pyridine nuclei contributed to heightened antiproliferative activity.

We also delved into investigating the impact of the selected compounds on the cell cycle of Capan-1 tumor cells to gain further insights into their underlying biological mechanisms. Furthermore, all synthesized compounds underwent testing for their antioxidative activity using established assays. A majority of the tested compounds exhibited significant antioxidative activity, particularly when assessed through the FRAP method. Notably, their antioxidative activity surpassed that of the standard BHT included in the study.

Computational analysis at the (SMD)/B3LYP/6–31+G(d) level elucidated hydroxy groups at the phenyl moiety as crucial structural elements in determining the antioxidant features of the prepared conjugates. This is based on their electron-donating ability to provide electronic density to the rest of the system, thereby allowing more efficient electron ionizations, but also on their H$^{\bullet}$ releasing tendency that surpasses that from the imidazole N–H group. Interestingly, due to steric crowding, the electron-donating features are optimal in dihidroxy derivatives, which are identified as potent antioxidants in FRAP assay where electron transfer reactions are dominant. In contrast, in trihidroxy derivatives, their ability to release hydrogen atoms and form a stable O–H·····O$^{\bullet}$·····H–O fragment upon H$^{\bullet}$ abstraction prevails, making them the most active antioxidants in DPPH$^{\bullet}$ assays where such a reactivity is relevant. Another noteworthy finding is that substituents on the imidazo[4,5-*b*]pyridine core, either aryl or alkyl groups on the imidazole nitrogen, or bromine on the pyridine unit, are only marginally affecting the antioxidant parameters. Typically, these modifications led to lower activities compared to the unsubstituted analogues. As a result, such structural alterations should be approached cautiously or avoided in future studies, especially when aiming for strong antioxidant properties.

4. Experimental part

4.1. Chemistry

4.1.1. General methods

All chemicals and solvents used in this study were procured from commercial suppliers including Aldrich, Acros, and Fluka. Melting points were determined using an

SMP11 Bibby apparatus and were recorded without any corrections. NMR spectra were acquired from DMSO-d6 solutions, with TMS serving as the internal standard. The 1H and 13C NMR spectra were obtained using various spectrophotometers: Varian Bruker Avance III HD 400 MHz/54 mm Ascend, Bruker AV300, or Bruker AV600 at frequencies of 300, 400, 600, 150, 100, and 75 MHz, respectively. Chemical shifts are reported in ppm (δ) relative to TMS. Compounds were routinely examined by thin-layer chromatography using Merck silica gel 60F-254 plates, and the spots were visualized under UV light (254 nm). Column chromatography was conducted using Fluka silica gel (0.063-0.2 mm), with a glass column slurry-packed under gravity.

Preparation of compounds **7**–**9**, **14**–**16**, **21**–**24**, **33**, **37**, **41** and **45** was published in our previous work.

4-((3-nitropyridin-2-yl)amino)phenol **10**

Compound **10** was prepared from 1.630 g (10.00 mmol) 2-chloro-3-nitropyridine **1** and 3.340 g (30.00 mmol) 4-aminophenol in 10 mL of DMF. Reaction mixture was heated for 40 minutes at the temperature of 100 °C. After cooling down, reaction mixture was poured on 150 mL of water and product precipitated. Product 4-(3-nitropyridine-yl)amino)phenol **10** was isolated in the form of orange crystals (1.503 g, 74%). M.p. = 144 - 145 °C. ^{1}H NMR (600 MHz, DMSO): δ/ppm = 9.83 (s, 1H, OH), 9.36 (s, 1H, NH), 8.50 (dd, 1H J_1 = 8.31, J_2 = 1.74 Hz, H_{arom}), 8.44 (dd, 1H, J_1 = 4.41, J_2 = 1.74 Hz, H_{arom}), 7.37 - 7.34 (m, 2H, H_{arom}), 6,89 (dd, 1H, J = 8.34, J_2 = 4.44 Hz, H_{arom}), 6.78 - 6.75 (m, 2H, H_{arom}); ^{13}C NMR (151 MHz, DMSO): δ/ppm = 155.94, 155.04, 150.71, 135.97, 129.96, 128.47, 125.71, 115.56, 114.06. Anal. Calcd. for $C_{11}H_9N_3O_3$: C, 57.14; H, 3.92; N, 18.17. Found: C, 56.84; H, 3.98; N, 18.14.

5-bromo-N-methyl-3-nitropyridin-2-amine **11**

3,000 g of 5-bromo-2-chloro-3-nitropyridine was dissolved in 120 mL of ethanol. Reaction mixture was cooled down in ice bath to 0 °C. 4.72 mL (37.90 mmol) of methylamine was added dropwise. Reaction mixture was stirred for 1 hour and the product was filtered off. 5-bromo-*N*-methyl-3-nitropyridine was isolated in the form of yellow crystals (2.581 g, 88%).

M.p. = 150 - 152 °C. ^{1}H NMR (600 MHz, DMSO): δ/ppm = 8.59 (d, 1H, J = 2.34 Hz, H_{arom}), 8.56 (d, 1H, J = 3.90 Hz, H_{arom}), 8.54 (d, 1H, J = 2.34 Hz, NH), 3.02 (d, 3H J = 4.74 Hz, CH_3); ^{13}C NMR (151 MHz, DMSO): δ/ppm = 155.60, 150.52, 135.77, 127.36, 102.48, 27.85. Anal. Calcd. for $C_6H_6BrN_3O_2$: C, 48.43; H, 3.48; N, 18.15. Found: C, 48.37; H, 3.53; N, 18.05

4-((5-bromo-3-nitropyridin-2-yl)amino)phenol **12**

2.000 g of 5-bromo-2-chloro-3-nitropyridine was dissolved in 80 mL of ethanol. Reaction mixture was cooled down in ice bath to 0 °C. 2.760 g (25.27 mmol) of 4-aminophenol was added. Reaction mixture was stirred for 4 hours and the product was filtered off. Product was isolated after column chromatography on SiO_2 using CH_2Cl_2/MeOH as eluens in form of purple crystals (1.440 g, 55 %). M.p. = 186 - 188 °C. ^{1}H NMR (600 MHz, DMSO): δ/ppm = 9.83 (s, 1H, OH), 9.40 (s, NH), 8.63 (d, 1H, *J* = 2.34 Hz, H_{arom}), 8.53 (d, 1H, *J* = 2.34 Hz, H_{atom}), 7.32 – 7.30 (m, 2H, H_{arom}), 6.77 – 6.75 (m, 2H, H_{arom}); ^{13}C NMR (151 MHz, DMSO): δ/ppm = 156.06, 155.34, 149.55, 137.21, 129.57, 128.93, 126.03, 115.60, 105.54. Anal. Calcd. for $C_{11}H_8BrN_3O_3$: C, 42.60; H, 2.60; N, 13.55. Found: C, 42.50; H, 2.63; N, 13.61

4.1.2. General procedure for the syntesis of amino-substituted pyridines

Solution of nitro-substituted pyridines **17**, **19**–**20** was refluxed with $SnCl_2{\times}2H_2O$ for half an hour. After cooling, solvent was removed and water was added to the reaction mixture. Solution was treated with 20% NaOH to pH 14 and extracted with ethyl-acetate.

4-((3-aminopyridin-2-yl)amino)phenol **17**

Compound **17** was prepared according to the general procedure by refluxing the solution of compound **10** (1.000 g, 4.33 mmol) in mixture of 20 mL of methanol and 20 mL of HCl and 3.908 g (17.32 mmol) of $SnCl_2 \times 2H_2O$ to obtain the product in form of brown crystals (0.718 g, 83%). M.p. = 222 - 226 °C. ^{1}H NMR (600 MHz, DMSO): δ/ppm = 8.86 (s, 1H, OH), 7.41 – 7.39 (m, 2H, NH, H_{arom}), 7.39 – 737 (m, 2H, H_{arom}), 6.82 (dd, 1H, J_1, = 7.47, J_2 = 1.62 Hz, NH), 6.71 – 6.63 (m, 2H, H_{arom}), 6.51 (dd, 1H, J_1 = 7.50, J_2 = 4.86 Hz, H_{arom}), 4.94 (s, 2H, NH_2); ^{13}C NMR (151 MHz, DMSO): δ/ppm = 151.84, 145.18, 134.85, 134.27, 131.42, 121.15, 119.36, 115.31, 114.90. Anal. Calcd. for $C_{11}H_{11}N_3O$: C, 65.66; H, 5.51; N, 20.88. Found: C, 65.73; H, 5.57; N, 20.75.

5-bromo-N^2-methylpyridine-2,3-diamine **19**

Compound **19** was prepared according to the general procedure by refluxing the solution of compound **11** (1.000 g, 4.31 mmol) in 25 mL of ethanol and 3.900 g (17.24 mmol) of $SnCl_2 \times 2H_2O$ to obtain the product in form of red oily crystals (0.752 g, 86%). M.p. = 107 - 110 °C. ^{1}H NMR (600 MHz, DMSO): δ/ppm = 7.39 (d, 1H, *J* = 2.16 Hz, H_{arom}), 6.78 (d, 1H, *J* = 2.16 Hz, H_{arom}), 5.82 (d, 1H, *J* = 4.38 Hz, NH), 4.98 (s, 2H, NH_2), 2.80 (d, 3H, *J* = 4.68 Hz, CH_3); ^{13}C NMR (151 MHz, DMSO): δ/ppm = 147.79, 134.44, 132.76, 118.52, 106.42, 28.58. Anal. Calcd. for $C_6H_8BrN_3$: C, 55.63; H, 5.00; N, 20.85. Found: C, 55.58; H, 5.01; N, 20.87.

4-((3-amino-5-bromopyridin-2-yl)amino)phenol **20**

Compound **20** was prepared according to the general procedure by refluxing the solution of compound **12** (1.330 g, 4.64 mmol) in 25 mL of ethanol and 4.188 g (18.56 mmol) of $SnCl_2 \times 2H_2O$ to obtain the product in form of beige powder (1.190 g, 92%). M.p. = 138 - 140 °C. ^{1}H NMR (600 MHz, DMSO): δ/ppm = 8.94 (s, 1H, OH), 7.55 (s, 1H, NH), 7.41 (d, 1H, *J* = 2.16 Hz, H_{arom}), 7.38 – 7.32 (m, 2H, H_{arom}), 6.95 (d, 1H, *J* = 2.22 Hz, H_{arom}), 6.70 – 6.64 (m, 2H, H_{arom}), 5.31 (s, 2H, NH_2); ^{13}C NMR (151 MHz, DMSO): δ/ppm = 152.35, 143.97, 133.88 133.47, 133.46, 121.62, 120.22, 115.39 108.45. Anal. Calcd. for $C_{11}H_{10}BrN_3O$: C, 65.66; H, 5.51; N, 20.88. Found: C, 65.69; H, 5.49; N, 20.79

4.1.3. General method for preparation of compounds 25-28

Solution of corresponding 2,3-diaminopyridine in ethyl-cyanoacetate was heated in oil bath at 190 °C. Reaction mixture was, after cooling, treated with diethyl-ether and product precipitated. Product was separated by filtration.

2-(3-(4-hydroxyphenyl)-3H-imidazo[4,5-b]pyridin-2-yl)acetonitrile **25**

Compound **25** was prepared according to the general procedure from 0.720 g (3.50 mmol) of **17** and 0.56 mL (5.20 mmol) of ethyl-cyanoacetate to obtain product in the form of brown powder (0.328 g, 66%). M.p. = 290 - 293 °C. ^{1}H NMR (600 MHz, DMSO): δ/ppm = 9.97 (s, 1H, OH), 8.30 (dd, 1H, J_1 = 4.74, J_2 = 1.32 Hz, H_{arom}), 8.16 (dd, 1H, J_1 = 8.01, J_2 = 1.32 Hz, H_{arom}), 7.36 – 7.33 (m, 3H, H_{arom}), 6.97 – 6.94 (m, 2H, H_{arom}), 4.35 (s, 2H, CH_2); ^{13}C NMR (151 MHz, DMSO): δ/ppm = 158.59, 149.40, 147.72, 144.68, 134.16, 129.38, 127.48, 124.79, 119.37, 116.50, 116.26, 19.15. Anal. Calcd. for $C_{14}H_{10}N_4O$: C, 67.19; H, 4.03; N, 22.39. Found: C, 67.25; H, 3.98; N, 22.45

2-(6-bromo-3H-imidazo[4,5-b]pyridin-2-yl)acetonitrile **26**

Compound **26** was prepared according to the general procedure from 1.000 g (5.32 mmol) of commercially available 5-bromo-2,3-diaminopyridine and 0.85 mL (7.98 mmol) of ethyl-cyanoacetate to obtain product in the form of orange powder (0.660 g, 52%). M.p. = 255 - 256 °C. ^{1}H NMR (600 MHz, DMSO): δ/ppm = 13.29 (bs, 1H, NH), 8.42 (s, 1H, H_{arom}), 8.30 (s, 1H, H_{arom}), 4.47 (s, 2H, CH_2); ^{13}C NMR (151 MHz, DMSO) δ/ppm = 143.53, 115.40, 112.36, 18.26. Anal. Calcd. for $C_8H_5BrN_4$: C, 40.53; H, 2.13; N, 23.63. Found: C, 40.60; H, 2.14; N, 23.57

2-(6-bromo-3-methyl-3H-imidazo[4,5-b]pyridin-2-yl)acetonitrile **27**

Compound **27** was prepared according to the general procedure from 0.737 g (3.65 mmol) of **19** and 0.58 mL (5.47 mmol) of ethyl-cyanoacetate to obtain product in the form of brown

powder (0.644 g, 71%). M.p. = 165 - 170 °C. ^{1}H NMR (600 MHz, DMSO): δ/ppm = 8.46 (d, 1H, *J* = 2.04 Hz, H_{arom}), 8.39 (d, 1H, *J* = 2.04 Hz, H_{arom}), 4.63 (s, 2H, CH_2), 3.75 (s, 3H, CH_3); ^{13}C NMR (151 MHz, DMSO): δ/ppm = 149.90, 147.45, 144.33, 135.53, 129.30, 118.56, 116.14, 113.53, 29.00, 18.63. Anal. Calcd. for $C_9H_7BrN_4$: C, 43.05; H, 2.81; N, 22.31. Found: C, 42.90; H, 2.78; N, 22.37.

2-(6-bromo-3-(4-hydroxyphenyl)-3H-imidazo[4,5-b]pyridin-2-yl)acetonitrile **28**

Compound **27** was prepared according to the general procedure from 1.180 g (4.19 mmol) of **28** and 0.67 mL (6.29 mmol) of ethyl-cyanoacetate to obtain product in form of grey powder (0.644 g, 49%).M.p. = 229 - 231 °C. ^{1}H NMR (600 MHz, DMSO): δ/ppm = 10.00 (s, 1H, OH), 8.48 (d, 1H, *J* = 2.04 Hz, H_{arom}), 8.40 (d, 1H, *J* = 2.10 Hz, H_{arom}), 7.35 (d, 2H, *J* = 8.70 Hz, H_{arom}), (d, 2H, *J* = 7.70 Hz, H_{arom}), 4.37 (s, 2H, CH_2); ^{13}C NMR (151 MHz, DMSO): δ/ppm = 157.71, 148.49, 147.15, 143.87, 134.35, 128.69, 128.25, 123.23, 115.46, 114.97, 113.01, 18.21. Anal. Calcd. for $C_{14}H_9BrN_4O$: C, 51.09; H, 2.76; N, 17.02. Found: C, 51.00; H, 2.80; N, 16.99.

4.1.4. General method for preparation of compounds 34-36, 38-40, 42-44 and 46-64

2-cyanomethylimidazo[4,5-*b*]pyridine **21-28** and equimolar amount of corresponding benzaldehyde **29-32** were dissolved in absolute ethanol. Two drops of piperidine were added to the solution and reaction mixture was refluxed for 2 hours. After cooling, product was filtered off and, if necessary, recrystallized.

(E)-3-(4-hydroxyphenyl)-2-(3H-imidazo[4,5-b]pyridin-2-yl)acrylonitrile **34**

Compound **34** was prepared according to the general procedure from 0.100 g (0.63 mmol) of **21** and 0.077 g (0.63 mmol) **30** in 5 mL of ethanol. After 2 hours product was isolated as yellow powder (0.114 g, 69%). M.p. = > 300 °C. ^{1}H NMR (400 MHz, DMSO): δ/ppm = 13.43 (bs, 1H, NH), 10.67 (bs, 1H, OH), 8.37 (dd, 1H, J_1 = 4.92, J_2 = 1.24 Hz, H_{arom}), 8.30 (s, 1H, CH), 8.03 (d, 1H, *J* = 7.60 Hz, H_{arom}), 7.93 (d, 2H, *J* = 8.76 Hz, H_{arom}), 7,27 (dd, 1H, J_1 = 8.00, J_2 = 4.76 Hz, H_{arom}), 7.01 – 6.96 (m, 2H, H_{arom}); ^{13}C NMR (151 MHz, DMSO): δ/ppm = 161.46, 146.69, 132.39, 123.62, 118.39, 116.57, 116.34. Anal. Calcd. for $C_{15}H_{10}N_4O$: C, 68.69; H, 3.84; N, 21.36. Found: C, 68.78; H, 3.88; N, 21.25.

(E)-3-(3,4-dihydroxyphenyl)-2-(3H-imidazo[4,5-b]pyridin-2-yl)acrylonitrile **35**

Compound 35 was prepared according to the general procedure from 0.100 g (0.63 mmol) of 21 and 0.087 g (0.63 mmol) of 31 in 5 mL of ethanol.

After 2 hours product was isolated as orange powder (0.112 g, 63%). M.p. = >250 °C. ^{1}H NMR (400 MHz, DMSO): δ/ppm = 8.36 (dd, 1H, J_1 = 4.76, J_2 = 1.32 Hz, H_{arom}), 8.20 (s, 1H, CH), 8.02 (d, 1H, J = 7.40 Hz, H_{arom}), 7.61 (d, 1H, J = 2.16 Hz, H_{arom}), 7.34 (dd, 1H, J_1 = 8.38, J_2 = 2.12 Hz, H_{arom}), 7.27 (dd, 1H, J_1 = 8.00, J_2 = 4.80 Hz, H_{arom}), 6.93 (d, 1H, J = 8.28, H_{arom}); ^{13}C NMR (151 MHz, DMSO): δ/ppm = 150.68, 150.16, 146.94, 145.82, 144.24, 124.60, 123.91, 118.33, 116.59, 116.08, 115.81, 96.76. Anal. Calcd. for $C_{15}H_{10}N_4O_2$: C, 64.74; H, 3.62; N, 20.13. Found: C, 64.80; H, 3.59; N, 20.01.

(E)-2-(3H-imidazo[4,5-b]pyridin-2-yl)-3-(3,4,5-trihydroxyphenyl)acrylonitrile **36**

Compound **36** was prepared according to the general procedure from 0.100 g (0.63 mmol) of **21** and 0.087 g (0.63 mmol) of **32** in 5 mL of ethanol. After 2 hours product was isolated as orange powder (0.164 g, 88%). M.p. = >300 °C. ^{1}H NMR (400 MHz, DMSO): δ/ppm = 9.62 (bs, 2H, OH), 8.35 (dd, 1H, J_1 = 4.88, J_2 = 1.16 Hz, H_{arom}), 8.10 (s, 1H, CH), 8.01 (d, 1H, J = 7.64 Hz, H_{arom}), 7.26 (dd, 2H, J_1 = 7.98, J_2 = 4.76 Hz, H_{arom}), 7.10 (s, 1H, CH); ^{13}C NMR (151 MHz, DMSO): δ/ppm = 150.44, 147.17, 146.13, 144.10, 139.99, 122.18, 118.24, 116.71, 109.70, 96.01. Anal. Calcd. for $C_{15}H_{10}N_4O_3$: C, 61.22; H, 3.43; N, 19.04. Found: C, 61.15; H, 3.45; N, 18.97.

(E)-3-(4-hydroxyphenyl)-2-(3-methyl-3H-imidazo[4,5-b]pyridin-2-yl)acrylonitrile **38**

Compound **38** was prepared according to the general procedure from 0.100 g (0.58 mmol) of **22** and 0.071 g (0.58 mmol) of **30** in 2 mL of ethanol. After 2 hours product was isolated as yellow powder (0.113 g, 71%). M.p. = 262 – 264 °C. ^{1}H NMR (400 MHz, DMSO): δ/ppm = 10.59 (bs, 1H, OH), 8.42 (dd, 1H, J_1 = 4.72, J_2 = 1.36 Hz, H_{arom}), 8.15 (s, 1H, CH), 8.11 (dd, 1H, J_1 = 7.98, J_2 = 1.36 Hz, H_{arom}), 8.01 (d, 2H, J = 8.80 Hz, H_{arom}), 7.35 (dd, 1H, J_1 = 7.98, J_2 = 4.72 Hz, H_{arom}), 6.98 (d, 2H, J = 8.70 Hz, H_{arom}), 4.03 (s, 3H, CH_3); ^{13}C NMR (151 MHz, DMSO): δ/ppm = 161.57, 150.60, 149.20, 148.43, 144.16, 134.11, 132.60, 126.77, 123.73, 118.89, 117.19, 116.80, 99.50, 95.48, 30.08. Anal. Calcd. for $C_{16}H_{12}N_4O$: C, 69.55; H, 4.38; N, 20.28. Found: C, 69.60; H, 4.37; N, 20.31.

(E)-3-(3,4-dihydroxyphenyl)-2-(3-methyl-3H-imidazo[4,5-b]pyridin-2-yl)acrylonitrile **39**

Compound **39** was prepared according to the general procedure from 0.100 g (0.58 mmol) of **22** and 0.080 g (0.58 mmol) of **31** in 2 mL of ethanol. After 2 hours product was isolated as orange powder (0.124 g, 73%). M.p. = 263 - 265 °C. ^{1}H NMR (400 MHz, DMSO): δ/ppm = 9.88 (bs, 1H, OH), 8.42 (dd, 1H, J_1= 4.74, J_2 =1.44 Hz, H_{arom}), 8.11 (dd, 1H, J_1= 8.00, J_2 = 1.44 Hz, H_{arom}), 8.05 (s, 1H, CH), 7.68 (d, 1H, J = 2.20 Hz, H_{arom}), 7.41 (dd, 1H, J_1 = 8.50, J_2 = 2.20 Hz, H_{arom}), 7.35 (dd, 1H, J_1= 8.00, J_2 = 4.,76 Hz, H_{arom}), 6.93 (d, 1H, J = 8.38 Hz,

H_{arom}), 4.02 (s, 3H, CH_3); ^{13}C NMR (151 MHz, DMSO): δ/ppm = 150.93, 150.69, 149.39, 148.45, 145.71, 144.07, 134.12, 126.70, 125.02, 124.07, 118.84, 117.19, 115.90, 115.84, 94.83, 30.07. Anal. Calcd. for $C_{16}H_{12}N_4O_2$: C, 65.75; H, 4.14; N, 19.17. Found: C, 65.80; H, 4.10; N, 19.20.

(E)-2-(3-methyl-3H-imidazo[4,5-b]pyridin-2-yl)-3-(3,4,5-trihydroxyphenyl)acrylonitrile **40**

Compound **40** was prepared according to the general procedure from 0.100 g (0.58 mmol) of **22** and 0.090 g (0.58 mmol) of **32** in 2 mL of ethanol. After 2 hours product was isolated as yellow powder (0.120 g, 67%). M.p. = 264 - 265 °C. ^1H NMR (400 MHz, DMSO): δ/ppm = 9.44 (bs, 2H, OH), 8.41 (dd, 1H, J_1 = 4.74, J_2 = 1.40 Hz, H_{arom}), 8.10 (dd, 1H, J_1 = 8.02, J_2 = 1.40 Hz, H_{arom}), 7.93 (s, 1H, CH), 7.35 (dd, 1H, J_1 = 8.00, J_2 = 4.76 Hz, H_{arom}), 7.15 (s, 2H, H_{arom}), 4.01 (s, 3H, CH_3); ^{13}C NMR (75 MHz, DMSO): δ/ppm = 151.31, 146.01, 144.02, 139.17, 126.65, 122.75, 118.82, 117.92, 109.95, 99.50, 99.48, 94.63, 30.06. Anal. Calcd. for $C_{16}H_{12}N_4O_3$: C, 62.33; H, 3.92; N, 18.17. Found: C, 62.29; H, 3.90; N, 18.17.

(E)-3-(4-hydroxyphenyl)-2-(3-isobutyl-3H-imidazo[4,5-b]pyridin-2-yl)acrylonitrile **42**

Compound **42** was prepared according to the general procedure from 0.050 g (0.23 mmol) of **23** and 0.028 g (0.23 mmol) of **30** in 5 mL of ethanol. After 2 hours product was isolated as yellow powder crystals (0.036 g, 49%). M.p. = 186 - 188 °C. ^1H NMR (600 MHz, DMSO): δ/ppm = 10.62 (s, 1H, OH), 8.42 (dd, 1H, J_1 = 4.74, J_2 = 1.38 Hz, H_{arom}), 8.25 (s, 1H, CH), 8.12 (dd, 1H, J_1 = 8.01, J_2 = 1.41 Hz, H_{arom}), 8.00 (d, 2H, J = 8.70 Hz, H_{arom}), 7.36 (dd, 1H, J_1 = 8.01 , J_2 = 4.71 Hz, H_{arom}), 6.98 (d, 2H, J = 8.70 Hz, H_{arom}), 4.42 (d, 2H, J = 7.56 Hz, CH_2), 2.28 - 2.24 (m, 1H, CH), 0.82 (d, 6H, J = 6.66 Hz, CH_3). ^{13}C NMR (151 MHz, DMSO): δ/ppm = 162.21, 151.92, 149.03, 148.92, 144.75, 134.33, 133.21, 127.42, 124.19, 119.52, 117.66, 116.73, 95.41, 49.99, 29.26, 20.06. Anal. Calcd. for $C_{19}H_{18}N_4O$: C, 71.68; H, 5.70; N, 17.60. Found: C, 71.71; H, 5.70; N, 17.66.

(E)-3-(3,4-dihydroxyphenyl)-2-(3-isobutyl-3H-imidazo[4,5-b]pyridin-2-yl)acrylonitrile **43**

Compound **43** was prepared according to the general procedure from 0.100 g (0.47 mmol) of **23** and 0.064 g (0.47 mmol) of **31** in 5 mL of ethanol. After 2 hours product was isolated as yellow crystals (0.070 g, 45%). M.p. = 140 - 142 °C. ^1H NMR (600 MHz, DMSO): δ/ppm = 10.13 (s, 1H, OH), 9.63 (s, 1H, OH), 8.41 (dd, 1H, J_1 = 4.71, J_2 = 1.41 Hz, H_{arom}), 8.13 (s, 1H, CH), 8.12 (dd, 1H, J_1 = 7.98, J_2 = 1.44 Hz, H_{arom}), 7.67 (d, 1H, J = 2.22 Hz, H_{arom}), 7.40 (dd, 1H, J_1 = 8.46, J_2 = 2.16 Hz, H_{arom}), 6.92 (d, 2H, J = 8.28 Hz, H_{arom}), 4.41 (d, 2H, J = 7.56 Hz, CH_2), 2.28-2.24 (m, 1H, CH), 0.82 (d, 6H, J = 6.66 Hz, CH_3). ^{13}C NMR (151 MHz, DMSO): δ/ppm = 152.20, 151.20, 149.10, 149.03, 146.23, 144.69, 134.35, 127.38, 125.65, 124.59,

119.49, 117.65, 116.45, 116.35, 94.93, 49.99, 29.24, 20.07. Anal. Calcd. for $C_{19}H_{18}N_4O_2$: C, 68.25; H, 5.43; N, 16.76. Found: C, 68.22; H, 5.42; N, 16.81.

(E)-2-(3-isobutyl-3H-imidazo[4,5-b]pyridin-2-yl)-3-(3,4,5-trihydroxyphenyl)acrylonitrile **44**

Compound **44** was prepared according to the general procedure from 0.060 g (0.28 mmol) of **23** and 0.043 g (0.28 mmol) of **32** in 1.5 mL of ethanol. After 2 hours product was isolated as red powder (0.020 g, 20%). M.p. = 165 - 167 °C. ^{1}H NMR (600 MHz, DMSO): δ/ppm = 8.28 (dd, 1H, J_1 = 4.77, J_2 = 1.35 Hz, H_{arom}), 7.97 (dd, 1H, J_1 = 7.89, J_2 = 1.35 Hz, H_{arom}), 7.89 (s, 1H, CH), 7.25 (dd, 1H, J_1 = 7.89, J_2 = 4.77 Hz, H_{arom}), 7.07 (s, 2H, H_{arom}), 6.52 (s, 2H, H_{arom}), 4.39 (d, 2H, J = 7.56 Hz, CH_2), 2.25 (m, 1H, CH), 0.82 (d, 6H, J = 6.66 Hz, CH_3).^{13}C NMR (151 MHz, DMSO): δ/ppm = 169.29, 151.19, 149.44, 147.20, 146.76, 143.22, 134.67, 125.96, 118.92, 109.89, 109.00, 52.27, 49.69, 26.49, 23.30, 20.05. Anal. Calcd. for $C_{19}H_{18}N_4O_3$: C, 65.13; H, 5.18; N, 15.99. Found: C, 64.98; H, 5.17; N, 16.04.

(E)-3-(4-hydroxyphenyl)-2-(3-phenyl-3H-imidazo[4,5-b]pyridin-2-yl)acrylonitrile **46**

Compound **46** was prepared according to the general procedure from 0.100 g (0.43 mmol) of **24** and 0.052 g (0.43 mmol) of **30** in 5 mL of ethanol. After 2 hours product was isolated as dark yellow powder (0.105 g, 73%). M.p. = 262 - 263 °C. ^{1}H NMR (300 MHz, DMSO): δ/ppm = 10.47 (s, 1H, OH), 8.35 (dd, 1H, J_1 = 4.73, J_2 = 1.34 Hz, H_{arom}), 8.22 (dd, 1H, J_1 = 8.03, J_2 = 1.30 Hz, H_{arom}), 7.82 (s, 1H, CH), 7.74 (d, 2H, J = 8,76 Hz, H_{arom}), 7.62 – 7.61(m, 5H, H_{arom}), 7.41 (dd, 1H, J_1 = 8.06, J_2 = 4.75 Hz, H_{arom}), 6.90 (d, 2H, J = 8.73 Hz, H_{arom}).^{13}C NMR (151 MHz, DMSO): δ/ppm = 161.62, 150.88, 149.00, 148.51, 144.81, 134.31, 134.10, 132.42, 129.59, 129.27, 128.13, 127.17, 123.43, 119.63, 116.20, 116.03, 95.45. Anal. Calcd. for $C_{21}H_{14}N_4O$: C, 74.54; H, 4.17; N, 16.56. Found: C, 74.55; H, 4.21; N, 16.60.

(E)-3-(3,4-dihydroxyphenyl)-2-(3-phenyl-3H-imidazo[4,5-b]pyridin-2-yl)acrylonitrile **47**

Compound **47** was prepared according to the general procedure from 0.100 g (0.43 mmol) of **24** and 0.059 g (0.43 mmol) of **31** in 5 mL of ethanol. After 2 hours product was isolated as dark yellow powder (0.095 g, 63%). M.p. = 138 - 140 °C. ^{1}H NMR (300 MHz, DMSO): δ/ppm = 8.34 (dd, 1H, J_1 = 4.68, J_2 = 1.23 Hz, H_{arom}), 8.20 (dd, 1H, J_1 = 7.99, J_2 =1.25 Hz, H_{arom}), 7.67 (s, 1H, CH), 7.63 – 7.58 (m, 5H, H_{arom}), 7.43 – 7.38 (m, 2H, H_{arom}), 7.10 (dd, 1H, J_1 = 8.38, J_2 =1.96 Hz, H_{arom}), 6.82 (d, 1H, J = 8.31 Hz, H_{arom}). ^{13}C NMR (75 MHz, DMSO): δ/ppm = 151.10, 150.82, 149.01, 148.72, 145.69, 144.73, 134.38, 134.12, 129.60, 129.23, 128.11, 127.10, 124.79, 123.69, 119.59, 116.09, 115.91, 115.59, 99.50, 99.48, 94.86. Anal. Calcd. for $C_{21}H_{14}N_4O_2$: C, 71.18; H, 3.98; N, 15.81. Found: C, 71.20; H, 4.00; N, 15.77.

(E)-2-(3-phenyl-3H-imidazo[4,5-b]pyridin-2-yl)-3-(3,4,5-trihydroxyphenyl)acrylonitrile **48**

Compound **48** was prepared according to the general procedure from 0.070 g (0.30 mmol) of **24** and 0.046 g (0.30 mmol) of **32** in 5 mL of ethanol. After 2 hours product was isolated as red powder (0.059 g, 54%). M.p. = 165 – 166 °C. ^{1}H NMR (300 MHz, DMSO): δ/ppm = 8.31 (dd, 1H, J_1 = 4.7, J_2 =1.38 Hz, H_{arom}), 8.17 (dd, 1H, J_1 = 8.03, J_2 = 1.36 Hz, H_{arom}), 7.67 – 7.52 (m, 5H, H_{arom}), 7.48 (s, 1H, CH), 7.39 (dd, 1H, J_1 = 8.00, J_2 = 4.75 Hz, H_{arom}), 6.84 (s, 2H, H_{arom}).^{13}C NMR (75 MHz, DMSO): δ/ppm = 151.14, 145.99, 144.46, 134.55, 129.58, 129.16, 128.12, 126.88, 119.49, 116.44, 109.59. Anal. Calcd. for $C_{21}H_{14}N_4O_3$: C, 68.10; H, 3.81; N, 15.13. Found: C, 68.07; H, 3.80; N, 15.09.

(E)-2-(3-(4-hydroxyphenyl)-3H-imidazo[4,5-b]pyridin-2-yl)-3-phenylacrylonitrile **49**

Compound **49** was prepared according to the general procedure from 0.100 g (0.40 mmol) of **25** and 0.042 g (0.40 mmol) of **30** in 5 mL of ethanol. After 2 hours product was isolated as yellow powder powder (0.035 g, 27%). M.p. = 245 – 246 °C. ^{1}H NMR (600 MHz, DMSO): δ/ppm = 10.00 (s, 1H, OH), 8.38 (dd, 1H, J_1 = 4.68, J_2 = 1.44 Hz, H_{arom}), 8.23 (dd, 1H, J_1 = 8.04, J_2 =1.44 Hz, H_{arom}), 7.98 (s, 1H, CH), 7.83 (dd, 2H, J = 7.56, 1.68 Hz, H_{arom}), 7.58 – 7.52 (m, 3H, H_{arom}), 7.42 (dd, 1H, J_1 =8.04, J_2 =4.68 Hz, H_{arom}), 7.42 (d, 2H, J =8.76 Hz, H_{arom}), 6.96 (d, 2H, J = 8.76 Hz, H_{arom}). ^{13}C NMR (151 MHz, DMSO): δ/ppm = 158.72, 151.37, 149.68, 148.44, 145.71, 134.45, 132.81, 132.65, 130.13, 129.87, 129.75, 127.95, 125.60, 120.13, 116.57, 115.77, 101.28. Anal. Calcd. for $C_{21}H_{14}N_4O$: C, 74.54; H, 4.17; N, 16.56. Found: C, 74.49; H, 4.17; N, 16.62.

(E)-3-(4-hydroxyphenyl)-2-(3-(4-hydroxyphenyl)-3H-imidazo[4,5-b]pyridin-2-yl)acrylonitrile **50**

Compound **50** was prepared according to the general procedure from 0.060 g (0.24 mmol) of **25** and 0.042 g (0.40 mmol) of **30** in 5 mL of ethanol. After 2 hours product was isolated as brown powder (0.057 g, 43%). M.p. = 223 – 227 °C. ^{1}H NMR (400 MHz, DMSO): δ/ppm = 8.29 (dd, 1H, J_1 = 4.72 Hz, J_2 = 1.32 Hz, H_{arom}), 8.14 (dd, 1H, J_1 = 8.00 Hz, J_2 = 1.36 Hz, H_{arom}), 7.77 (s, 1H, CH), 7.69 (d, 2H, J = 8.80 Hz, H_{arom}), 7.36 (dd, 1H, J_1 = 8.12 Hz, J_2 = 4.76 Hz, H_{arom}) 7.31 (d, 2H, J = 8.76 Hz, H_{arom}), 6.95 (d, 2H, J = 8.72 Hz, H_{arom}), 6.73 (d, 2H, J = 8.68 Hz, H_{arom}); ^{13}C NMR (101 MHz, DMSO): δ/ppm = 158.67, 150.84, 150.07, 149.94, 144.68, 134.64, 133.32, 129.88, 127.06, 125.91, 121.74, 119.74, 117.73, 117.25, 116.52. Anal. Calcd. for $C_{21}H_{14}N_4O_2$: C, 71.18; H, 3.98; N, 15.81. Found: C, 71.09; H, 3.99; N, 15.75.

(E)-3-(3,4-dihydroxyphenyl)-2-(3-(4-hydroxyphenyl)-3H-imidazo[4,5-b]pyridin-2-yl)acrylonitrile **51**

Compound **51** was prepared according to the general procedure from 0.060 g (0.24 mmol) of **25** and 0.033 g (0.24 mmol) of **31** in 5 mL of ethanol. After 2 hours product was isolated as orange powder (0.053 g, 38%). M.p. = 257 – 259 °C. ^{1}H NMR (400 MHz, DMSO): δ/ppm = 8.23 (dd, 1H, J_1 = 4.72 Hz, J_2 =1.32 Hz, H_{arom}), 8.07 (dd, 1H, J_1 = 7.96 Hz, J_1 = 1.32 Hz, H_{arom}), 7.56 (s, 1H, CH), 7.40 (d, 1H, J = 2.24 Hz, H_{arom}), 7.32 (dd, 1H, J_1 = 8.08, J_1 = 4.56 Hz, H_{arom}) 7.30 (d, 1H, J = 8.72 Hz, H_{arom}), 6.98-6.93 (m, 3H, H_{arom}), 6.47 (d, 2H, J = 8.40 Hz, H_{arom}); ^{13}C NMR (101 MHz, DMSO): δ/ppm = 158.51, 151.15, 150.69, 150.14, 147.72, 143.98, 134.82, 129.90, 129.01, 126.42, 126.27, 119.48, 118.16, 116.48, 116.04, 111.95. Anal. Calcd. for $C_{21}H_{14}N_4O_3$: C, 68.10; H, 3.81; N, 15.13. Found: C, 68.19; H, 3.80; N, 15.17.

(E)-2-(3-(4-hydroxyphenyl)-3H-imidazo[4,5-b]pyridin-2-yl)-3-(3,4,5-trihydroxyphenyl) acrylonitrile **52**

Compound **52** was prepared according to the general procedure from 0.100 g (0.40 mmol) of **25** and 0.062 g (0.40 mmol) of **32** in 5 mL of ethanol. After 2 hours product was isolated as dark red powder powder (0.053 g, 42%). M.p. = 235 – 238 °C. ^{1}H NMR (600 MHz, DMSO): δ/ppm = 8.19 (dd, 1H, J_1 = 4.77, J_1 = 1.41 Hz, H_{arom}), 8.04 (dd, 1H, J_1 =7.92, J_1 =1.38 Hz, H_{arom}), 7.43 (s, 1H, CH), 7.29 (d, 2H, J = 8.70 Hz, H_{arom}), 7.28 (dd, 1H, J_1 = 7.98, J_2 = 4.86 Hz, H_{arom}), 6.94 (d, 2H, J = 8.70 Hz, H_{arom}), 6.82 (s, 2H, H_{arom}). ^{13}C NMR (151 MHz, DMSO): δ/ppm = 158.39, 151.47, 150.41, 150.22, 146.64, 143.75, 134.89, 129.90, 126.45, 126.20, 119.40, 118.50, 116.46, 109.64. Anal. Calcd. for $C_{15}H_{10}N_4O_3$: $C_{21}H_{14}N_4O_4$: C, 65.28; H, 3.65; N, 14.50. Found: C, 65.31; H, 3.68; N, 14.55.

(E)-2-(6-bromo-3H-imidazo[4,5-b]pyridin-2-yl)-3-phenylacrylonitrile **53**

Compound **53** was prepared according to the general procedure from 0.100 g (0.42 mmol) of **26** and 0.045 g (0.42 mmol) of **29** in 5 mL of ethanol. After 2 hours product was isolated as yellow powder (0.063 g, 46%). M.p. = 289 – 291 °C. ^{1}H NMR (600 MHz, DMSO): δ/ppm = 13.87 (bs, 1H, NH), 8.49 (d, 1H, J = 1.80 Hz, H_{arom}), 8.46 (s, 1H, H_{arom}), 8,37 (s, 1H, CH), 8.01 (dd, 2H, J_1 = 6.42, J_2 = 1.74 Hz, H_{arom}), 7.65 – 7.60 (m, 3H, H_{arom}); ^{13}C NMR (101 MHz, DMSO): δ/ppm = 150.98, 148.16, 145.74, 132.88, 132.74, 130.31, 129.89, 116.15. Anal. Calcd. for $C_{15}H_9BrN_4$: C, 55.41; H, 2.79; N, 17.23. Found: C, 55.43; H, 2.78; N, 17.19.

(E)-2-(6-bromo-3H-imidazo[4,5-b]pyridin-2-yl)-3-(4-hydroxyphenyl)acrylonitrile **54**

Compound **54** was prepared according to the general procedure from 0.100 g (0.42 mmol) of **26** and 0.050 g (0.42 mmol) of **30** in 5 mL of ethanol. After 2 hours product was isolated as light orange powder (0.081 g, 56%). M.p. > 300 °C. ^{1}H NMR (600 MHz, DMSO): δ/ppm = 13.68 (s, 1H, NH), 10.64 (s, 1H, OH), 8.44 (d, 1H, J = 1.68 Hz, H_{arom}), 8.31 (s, 1H, H_{arom}),

8.30 (s, 1H, CH), 7.93 (d, 2H, *J* = 8.64 Hz, H_{arom}), 6.99 (d, 2H, *J* = 8.76 Hz, H_{arom}); ^{13}C NMR (151 MHz, DMSO): δ/ppm = 162.19, 151.89, 148.00, 145.14, 133.01, 124.03, 116.93, 116.89, 113.77, 97.40. Anal. Calcd. for $C_{15}H_9BrN_4O$: C, 52.81; H, 2.66; N, 16.42. Found: C, 52.71; H, 2.69; N, 16.40.

(E)-2-(6-bromo-3H-imidazo[4,5-b]pyridin-2-yl)-3-(3,4-dihydroxyphenyl)acrylonitrile **55**

Compound **55** was prepared according to the general procedure from 0.100 g (0.42 mmol) of **26** and 0.058 g (0.42 mmol) of **31** in 5 mL of ethanol. After 2 hours product was isolated as orange powder (0.089 g, 59%). M.p. > 300 °C. ^1H NMR (600 MHz, DMSO): δ/ppm = 9.87 (bs, 1H, OH), 8.44 (d, 1H, *J* = 2.04 Hz, H_{arom}), 8.29 (s, 1H, H_{arom}), 8,22 (s, 1H, CH), 7.61 (d, 1H, *J* = 2.16 Hz, H_{arom}), 7.35 (dd, 1H, J_1 = 8.34, J_2 = 2.10 Hz, H_{arom}), 6.94 (d, 1H, *J* = 8.28 Hz, H_{arom}); ^{13}C NMR (151 MHz, DMSO): δ/ppm = 152.13, 151.26, 148.22, 146.32, 145.03, 125.33, 124.43, 116.92, 116.62, 116.45, 113.70, 96.92. Anal. Calcd. for $C_{15}H_9BrN_4O_2$: C, 50.44; H, 2.54; N, 15.69. Found: C, 50.55; H, 2.53; N, 15.76.

(E)-2-(6-bromo-3H-imidazo[4,5-b]pyridin-2-yl)-3-(3,4,5-trihydroxyphenyl)acrylonitrile **56**

Compound **56** was prepared according to the general procedure from 0.100 g (0.42 mmol) of **26** and 0.065 g (0.42 mmol) of **31** in 5 mL of ethanol. After 2 hours product was isolated as orange powder (0.067 g, 43%). M.p. > 300 °C. ^1H NMR (600 MHz, DMSO): δ/ppm = 9.54 (bs, 2H, OH), 8.43 (d, 1H, *J* = 2.04 Hz, H_{arom}), 8.28 (s, 1H, H_{arom}), 8.12 (s, 1H, H_{arom}), 7.10 (s, 2H, H_{arom});

^{13}C NMR (151 MHz, DMSO): δ/ppm = 152.24, 148.52, 146.62, 144.98, 139.65, 123.18, 116.89, 113.67, 110.42, 96.83. Anal. Calcd. for $C_{15}H_9BrN_4O_3$: C, 48.28; H, 2.43; N, 15.01. Found: C, 48.37; H, 2.43; N, 14.95.

(E)-2-(6-bromo-3-methyl-3H-imidazo[4,5-b]pyridin-2-yl)-3-phenylacrylonitrile **57**

Compound **57** was prepared according to the general procedure from 0.070 g (0.28 mmol) of **27** and 0.031 g (0.28 mmol) of **29** in 5 mL of ethanol. After 2 hours product was isolated as brown powder (0.036 g, 38%). M.p. = 192 - 193 °C. ^1H NMR (600 MHz, DMSO): δ/ppm = 8.55 (d, 1H, *J* = 2.04 Hz, H_{arom}), 8.46 (d, 1H, *J* = 2.10 Hz, H_{arom}), 8.33 (s, 1H, CH), 8.07 (dd, 2H, J_1 = 6.66, J_2 = 3.60 Hz, H_{arom}), 7.63 – 7.61 (m, 3H, H_{arom}), 4.04 (s, 3H, CH_3); ^{13}C NMR (151 MHz, DMSO): δ/ppm = 151.79, 150.40, 147.73, 145.40, 135.67, 133.00, 132.78, 130.44, 129.85, 129.72, 116.75, 114.29, 101.03, 30.94. Anal. Calcd. for $C_{16}H_{11}BrN_4$: C, 56.66; H, 3.27; N, 16.52. Found: C, 56.72; H, 3.30; N, 16.47

(E)-2-(6-bromo-3-methyl-3H-imidazo[4,5-b]pyridin-2-yl)-3-(4-hydroxyphenyl)acrylonitrile **58**

Compound **58** was prepared according to the general procedure from 0.070 g (0.28 mmol) of **27** and 0.034 g (0.28 mmol) of **30** in 5 mL of ethanol. After 2 hours product was isolated as yellow powder (0.046 g, 46%). M.p. = 259 - 260 °C. ^{1}H NMR (600 MHz, DMSO): δ/ppm = 10.57 (bs, 1H, OH) 8.51 (d, 1H, *J* = 1.86 Hz, H_{arom}), 8.40 (d, 1H, *J* = 1.92 Hz, H_{arom}), 8.17 (s, 1H, CH), 8.00 (d, 2H, *J* = 8.70 Hz, H_{arom}), 6.97 (d, 2H, *J* = 8.70 Hz, H_{arom}), 4.01 (s, 3H, CH_3); ^{13}C NMR (151 MHz, DMSO): δ/ppm = 161.38, 150.57, 150.17, 146.75, 143.74, 134.70, 132.23, 128.30, 122.97, 116.49, 115.69, 94.36, 29.78. Anal. Calcd. for $C_{16}H_{11}BrN_4O$: C, 54.10; H, 3.12; N, 15.77. Found: C, 54.03; H, 3.09; N, 15.82.

(E)-2-(6-bromo-3-methyl-3H-imidazo[4,5-b]pyridin-2-yl)-3-(3,4-dihydroxyphenyl)acrylonitrile **59**

Compound **59** was prepared according to the general procedure from 0.070 g (0.28 mmol) of **27** and 0.039 g (0.28 mmol) of **31** in 5 mL of ethanol. After 2 hours product was isolated as yellow powder (0.037 g, 37%). M.p. = 267 - 269 °C. ^{1}H NMR (600 MHz, DMSO): δ/ppm = 9.42 (bs, 1H, OH), 8.50 (d, 1H, *J* = 2.04 Hz, H_{arom}), 8.39 (d, 1H. *J* = 2.04 Hz, H_{arom}), 8.06 (s, 1H, CH), 7.68 (d, 1H, *J* = 2.16 Hz, H_{arom}), 7.40 (dd, 1H, J_1 = 8.43, J_2 = 2.22 Hz, H_{arom}), 6.91 (d, 1H, *J* = 8.28 Hz, H_{arom}), 4.00 (s, 3H, CH_3); ^{13}C NMR (151 MHz, DMSO): δ/ppm = 151.97, 151.61, 151.46, 147.85, 146.28, 144.72, 135.81, 129.30, 125.90, 124.40, 117.58, 116.42, 114.06, 94.80, 30.86. Anal. Calcd. for $C_{16}H_{11}BrN_4O_2$: C, 51.77; H, 2.99; N, 15.09. Found: C, 51.82; H, 3.00; N, 15.13.

(E)-2-(6-bromo-3-methyl-3H-imidazo[4,5-b]pyridin-2-yl)-3-(3,4,5-trihydroxyphenyl)-acrylonitrile **60**

Compound **60** was prepared according to the general procedure from 0.070 g (0.28 mmol) of **27** and 0.043 g (0.28 mmol) of **31** in 5 mL of ethanol. After 2 hours product was isolated as dark red powder (0.056 g, 52%). M.p. > 300 °C. ^{1}H NMR (600 MHz, DMSO): δ/ppm = 8.35 (d, 1H, *J* = 2.10 Hz, H_{arom}), 8.21 (d, 1H, *J* = 2.04 Hz, H_{arom}), 7.81 (s, 1H, CH), 7.10 (s, 2H, H_{arom}), 3.95 (s, 3H, CH3); ^{13}C NMR (101 MHz, DMSO): δ/ppm = 153.73, 150.82, 148.26, 146.80, 143.01, 136.35, 127.71, 119.90, 116.97, 113.59, 110.07, 30.78. Anal. Calcd. for $C_{16}H_{11}BrN_4O_3$: C, 49.63; H, 2.86; N, 14.47. Found: C, 49.50; H, 2.87; N, 14.40.

(E)-2-(6-bromo-3-(4-hydroxyphenyl)-3H-imidazo[4,5-b]pyridin-2-yl)-3-phenylacrylonitrile **61**

Compound **61** was prepared according to the general procedure from 0.100 g (0.30 mmol) of **28** and 0.031 g (0.30 mmol) of **29** in 5 mL of ethanol. After 2 hours product was isolated as brown powder (0.038 g, 30%). M.p. = 219 - 221 °C**.** ^{1}H NMR (400 MHz, DMSO): δ/ppm = 8.54 (d, 1H, *J* = 2.08 Hz, H_{arom}), 8.47 (d, 1H, *J* = 2.08 Hz, H_{arom}), 8.01 (s, 1H, CH), 7.84 (dd, 2H, J_1 = 7.96 Hz, J_2 = 1.88 Hz, H_{arom}), 7.57 (d, 3H, *J* = 7.28 Hz, H_{arom}), 7.41 (d, 2H, *J* = 8.76 Hz, H_{arom}), 6.96 (d, 2H, *J* = 8.76 Hz, H_{arom}); ^{13}C NMR (101 MHz, DMSO): δ/ppm = 158.94, 151.99, 149.84, 148.53, 145.91, 135.67, 132.85, 132.68, 130.24, 130.05, 129.85, 129.77, 125.13, 116.62, 115.56, 114.80, 100.91. Anal. Calcd. for $C_{21}H_{13}BrN_4O$: C, 60.45; H, 3.14; N, 13.43. Found: C, 60.55; H, 3.12; N, 13.35.

(E)-2-(6-bromo-3-(4-hydroxyphenyl)-3H-imidazo[4,5-b]pyridin-2-yl)-3-(4-hydroxyphenyl)acrylonitrile **62**

Compound **62** was prepared according to the general procedure from 0.100 g (0.30 mmol) of **28** and 0.037 g (0.30 mmol) of **30** in 5 mL of ethanol. After 2 hours product was isolated as orange powder (0.037 g, 46%). M.p. = 238 - 240 °C. ^{1}H NMR (400 MHz, DMSO): δ/ppm = 8.30 (d, 1H, *J* = 2.04 Hz, H_{arom}), 8.27 (d, 1H, *J* = 2.08 Hz, H_{arom}), 7.56 (s, 1H, CH), 7.39 (d, 1H, *J* = 2.28 Hz, H_{arom}), 7.31 (d, 2H, *J* = 8.76 Hz, H_{arom}), 6.94 (d, 4H, *J* = 8.72 Hz, H_{arom}), 6.38 (d, 1H, *J* = 8.48 Hz, H_{arom}); ^{13}C NMR (101 MHz, DMSO): δ/ppm = 158.66, 153.27, 150.68, 148.02, 143.58, 136.31, 130.55, 129.92, 128.04, 125.96, 118.38, 116.51, 116.16, 114.13, 110.92. Anal. Calcd. for $C_{21}H_{13}BrN_4O_2$: C, 58.22; H, 3.02; N, 12.93. Found: C, 58.11; H, 3.02; N, 12.91.

(E)-2-(6-bromo-3-(4-hydroxyphenyl)-3H-imidazo[4,5-b]pyridin-2-yl)-3-(3,4-dihydroxy-phenyl)acrylonitrile **63**

Compound **63** was prepared according to the general procedure from 0.100 g (0.30 mmol) of **28** and 0.031 g (0.30 mmol) of **31** in 5 mL of ethanol. After 2 hours product was isolated as dark red powder (0.043 g, 32%). M.p. = 220- 223 °C. ^{1}H NMR (400 MHz, DMSO): δ/ppm = 8.42 (d, 1H, *J* = 2.00 Hz, H_{arom}), 8.37 (d, 1H, *J* = 2,00 Hz, H_{arom}), 7.80 (s, 1H, CH), 7.71 (s, 1H, H_{arom}), 7.69 (s, 1H, H_{arom}), 7.35 (d, 2H, *J* = 8.68 Hz, H_{arom}), 6,94 (d, 2H, *J* = 8.68 Hz, H_{arom}), 6.74 (d, 2H, *J* = 8.80 Hz, H_{arom}); ^{13}C NMR (101 MHz, DMSO): δ/ppm = 163.25, 161.90, 158.85, 156.16, 151.54, 151.31, 148.82, 144.78, 135.93, 133.51, 132.60, 129.88, 129.11, 125.46, 121.85, 117.74, 117.00, 116.56, 114.46. Anal. Calcd. for $C_{21}H_{13}BrN_4O_3$: C, 56.14; H, 2.92; N, 12.47. Found: C, 56.20; H, 2.92; N, 12.51.

(E)-2-(6-bromo-3-(4-hydroxyphenyl)-3H-imidazo[4,5-b]pyridin-2-yl)-3-(3,4,5-trihydroxy-phenyl)acrylonitrile **64**

Compound **64** was prepared according to the general procedure from 0.100 g (0.30 mmol) of **28** and 0.047 g (0.30 mmol) of **29** in 5 mL of ethanol. After 2 hours product was isolated as dark red powder (0.038 g, 27%). M.p. = 210 - 224 °C. ^{1}H NMR (400 MHz, DMSO): δ/ppm = 8.24 (d, 1H, *J* = 2.04 Hz, H_{arom}), 8.22 (d, 1H, *J* = 2,08 Hz, H_{arom}), 7.41 (s, 1H, CH), 7.29 (d, 2H, *J* = 8.76 Hz, H_{arom}), 6.94 (d, 2H, *J* = 8.68 Hz, H_{arom}), 6.81 (s, 1H, H_{arom}), 6.52 (s, 1H, H_{arom}); ^{13}C NMR (151 MHz, DMSO): δ/ppm = 169.26, 158.57, 150.15, 149.29, 147.17, 146.73, 143.24, 136.43, 129.93, 127.74, 126.14, 116.49, 114.04, 109.73, 109.03. Anal. Calcd. for $C_{21}H_{13}BrN_4O_4$: C, 54.21; H, 2.82; N, 12.04. Found: C, 54.11; H, 2.87; N, 12.07.

4.2. Biological activity

4.2.1. 2D proliferation assays

Adherent cell lines (Capan-1; MIA Paca-2; Panc-1; HCT-116; LN-229; NCI-H460) were seeded in 384-well tissue culture plates (Greiner) at a density between 500 and 1500 cells per well. Following an overnight incubation, cells were subjected to treatment with seven different concentrations of the test compounds, ranging from 100 to 0.006µM. Suspension cell lines (DND-41; HL-60; K-562; Z-138) were seeded in 384-well culture plates at densities ranging from 2500 to 5500 cells per well, and they were treated with the same concentrations of the test compounds. After a 72-hour incubation period, cell viability was assessed using the CellTiter 96® AQueous One Solution Cell Proliferation Assay (MTS reagent, Promega), following the manufacturer's protocol. Absorbance of the samples was measured at 490 nm using a SpectraMax Plus 384 (Molecular Devices), and the optical density (OD) values were utilized to calculate the 50% inhibitory concentration (IC_{50}). Compounds were tested in two independent experiments.

4.2.2. 3D proliferation assays

Pancreatic adenocarcinoma cell lines (Capan-1; MIA Paca-2; Panc-1) were seeded in 384-well PrimeSurface® 3D Culture Spheroid ULA Plates (S-BIO) at a density ranging from 200 to 500 cells per well. Following centrifugation, the plates were incubated at 37°C and continuously monitored using an IncuCyte® device (Essen BioScience Inc., Ann Arbor, MI, USA) for real-time imaging. Brightfield and phase images were captured every 12 hours, with one field imaged per well under 10x magnification. Upon reaching an average spheroid

diameter of 200 – 400 nm (day 3), the cells were treated with various concentrations of the test compounds. The plates were subjected to centrifugation and monitored for an additional 10 days. . Cell growth was quantified based on the average size of the spheroids, analyzed using the IncuCyte® image analysis software. The obtained data were used to determine the IC_{50} values. Compounds were tested in two independent experiments.

4.2.3. PBMC viability assay

Buffy coat preparations from healthy donors were obtained from the Blood Transfusion Center in Leuven, Belgium. Peripheral blood mononuclear cells (PBMC) were isolated through density gradient centrifugation over Lymphoprep (d=1.077 g/ml) (Nycomed, Oslo, Norway) and cultured in cell culture medium (DMEM/F12, Gibco Life Technologies, USA) supplemented with 8% FBS. Freshly prepared PBMC were seeded in 384-well culture plates containing the test compounds at different concentration points at a density of 28000 cells per well. Following a 72-hour incubation with the compounds, the cells were analyzed using the MTS reagent, following the manufacturer's instructions. The absorbance of the samples was measured at 490 nm using a SpectraMax Plus 384 (Molecular Devices), and OD values were used to calculate the 50% inhibitory concentration (IC_{50}). Compounds were tested in three independent experiments, which imply PBMC originated from three different donors.

4.2.4. Erythrocyte hemolysis assay

Biological antioxidative activity was evaluated by conducting an H_2O_2-induced erythrocyte hemolysis test. Chicken blood collected in EDTA vials was subjected to centrifugation for 10 minutes at 1800 rpm. The resulting supernatant was discarded, and the pellet underwent two washes with PBS before being resuspended in a 2% PBS solution. Test and reference compounds were appropriately diluted in PBS and added to the erythrocyte suspension, followed by a 15-minute incubation at room temperature. To induce oxidative degradation of membrane lipids, an H_2O_2 solution was introduced, and the mixtures were further incubated for 2 hours at 37°C. Subsequently, the samples underwent centrifugation at 1800 rpm for 10 minutes, and the absorbance of the supernatant was measured spectrophotometrically at 540 nm. The extent of hemolysis was evaluated relative to the hemolysis observed in the H_2O_2-treated negative control (PBS), which was designated as 100%. Compounds were tested in two independent experiments.

4.2.5. Cell cycle

Capan-1 cells were plated at a density of 10.000 cells per well in 96-well plates. Following an overnight incubation, the cells were exposed to the test compounds across six concentrations ranging from 100 to 0.3 µM and were then incubated for 24 hours. Subsequently, the cells were fixed using 4% paraformaldehyde (PFA) in PBS for 10 minutes, underwent a washing step, and had their nuclei stained with DAPI. Imaging of the plates was conducted using a CX5 High Content Screening device (ThermoFisher Scientific), employing the Cell Cycle Analysis bio-application. A minimum of 1000 cells per condition were subjected to analysis. Compounds were tested in two independent experiments.

4.3. Antioxidative activity

Determination of the reducing activity of the stable radical 1,1-diphenyl-picrylhydrazyl (DPPH)

The reducing activity of investigated systems was achieved by the DPPH method according to previously described procedures with modifications to assure the use in a 96-well microplate. Briefly, equal volumes of various concentrations of tested molecules (dissolved in DMSO) were added to the solution of DPPH (final concentration 50 µM in absolute ethanol). Ethanol and DMSO were used as control solutions in line with earlier reports.

Determination of Ferric Reducing/Antioxidant Power (FRAP assay)

The FRAP method was carried out according to previously described procedures with some modifications to be compatible with an assay on a 96-well microplate.
All results were expressed as Fe^{2+} equivalents (Fe^{2+} µmol). All tests were done in triplicate and the results were averaged and presented in Table 1.

ABTS Radical Scavenging Assay

The total antioxidant activity (TEAC) method was modified and adjusted for the microtiter plate reader. For the standard TEAC assay, $ABTS^{\bullet+}$ (2,2′-azino-bis(3-ethylbenzothiazoline-6-sulfonic acid) radical cation was prepared by mixing an ABTS stock solution (7 mM in water) with 2.45 mM potassium persulfate, which was allowed to stand for 12–16 h at room temperature in the dark until reaching a stable oxidative state. On the day of analysis, the $ABTS^{\bullet+}$ solution was diluted with PBS (pH 7.4) to an absorbance of 0.700 ± 0.01 at 734 nm. The radical was stable in this form for more than two days when stored in the dark at room temperature. Standards and solutions of tested compounds (10 µL) were mixed with working $ABTS^{\bullet+}$ (200 µL) in microplate wells and incubated at room temperature for 5 min. The decrease of absorbance at 734 nm was recorded by µQuant (Biotec Inc.). Aqueous

phosphate buffer solution and Trolox (0.20–1.25 mmol/L) were used as a control and a main calibrating standard, respectively. Results were expressed as average of three independent measure as trolox equivalents (mmol TEAC/ mmolC).

4.4. Computational Details

As a good compromise between accuracy and feasibility, all geometries were optimized with the density functional theory (DFT) using the B3LYP functional (unrestricted UB3LYP for the radicals), and the 6–31+G(d) basis set followed by the harmonic frequency calculations. Thermal corrections were extracted from the corresponding frequency calculations without scaling factors, while the obtained structures were confirmed as true minima by the absence of imaginary vibrational frequencies. In this way, all reported values correspond to differences in Gibbs free energies obtained at a room temperature (298 K) and a normal pressure (1 atm). To account for the solvation effects, we included the SMD polarizable continuum model with all parameters corresponding to pure ethanol ($\varepsilon = 24.852$), in accordance with presented experiments, giving rise to the (SMD)/B3LYP/6–31+G(d) model employed here. The choice of this computational setup was prompted by its success in modeling mechanisms of various antioxidants,[28, 37 – 40] and in reproducing kinetic and thermodynamic parameters of a variety of organic[41, 42] and enzymatic reactions.[43, 44] All calculations were performed using the Gaussian 16 software.[45]

According to the literature, there are multiple mechanisms that describe the antioxidative properties of molecules.[46–48] Here we evaluated the three most frequent, and usually thermodynamically most preferred antioxidant mechanisms, namely hydrogen atom transfer (HAT), related with the capacity to transfer the hydrogen atom ($H^{\bullet}$) to a free radical as governed by the M–H bond dissociation energy (BDE), and single electron transfer (SET) related with either ejecting or adding an electron to the system. All these mechanisms have the same net result, i.e. the formation of corresponding antioxidant radical and are calculated as Gibbs free energies for the following processes:

$\mathbf{M}\text{–H} \rightarrow \mathbf{M}^{\bullet} + H^{\bullet}$ [bond dissociation energy, $BDE = G(\mathbf{M}^{\bullet}) + G(H^{\bullet}) - G(\mathbf{M}\text{–H})$]

$\mathbf{M} \rightarrow \mathbf{M}^{\bullet+} + e^{-}$ [ionization energy, $IE = G(\mathbf{M}^{\bullet+}) - G(\mathbf{M})$]

$\mathbf{M} + e^{-} \rightarrow \mathbf{M}^{\bullet-}$ **[**electron affinity, $EA = G(\mathbf{M}^{\bullet-}) - G(\mathbf{M})$**]**

5. Acknowledgments

We greatly appreciate the financial support of the Croatian Science Foundation under the projects IP-2018-02-4379 and IP–2020–02–8090. R.V. wishes to thank the Zagreb University Computing Centre (SRCE) for granting computational resources on the ISABELLA cluster. D.D. and L.P. are grateful for excellent technical assistance by J. Punjwani, Y. Smolders, N. Van Winkel and N. Willems.

6. Conflict of interests

The authors declare no conflict of interest.

References

[1] J. Pokorný, Are natural antioxidants better – and safer – than synthetic antioxidants? Eur. J. Lipid Sci. Technol. 109 (2007) 629–642, https://doi.org/10.1002/ejlt.200700064.

[2] M. Stoia, S. Oancea, Low-Molecular-Weight Synthetic Antioxidants: Classification, Pharmacological Profile, Effectiveness and Trends, Antioxidants 11 (2022), 638, https://doi.org/10.3390/antiox11040638.

[3] J. Daintith, E. Martin, Oxford Dictionary of Science, 6th Edition, Oxford University Press, 2010.

[4] N. C. Charlton, M. Mastyugin, B. Török, M. Török, Structural Features of Small Molecule Antioxidants and Strategic Modifications to Improve Potential Bioactivity, Molecules 28(3) (2023) 1057, https://doi.org/10.3390/molecules28031057.

[5] C. Rice-Evans, N. Miller, G. Paganga, Antioxidant properties of phenolic compounds. Trends Plant Sci. 2 (1997) 152–159, https://doi.org/10.1016/S1360-1385(97)01018-2.

[6] C. A. Rice-Evans, N. J. Miller, G. Paganga, Structure-antioxidant activity relationships of flavonoids and phenolic acids, Free Radic. Biol. Med. (20) (1996) 933–956, https://doi.org/10.1016/0891-5849(95)02227-9.

[7] S. J. Padayatty, M. Levine, Vitamin C: The known and the unknown and Goldilocks, Oral Dis. 22 (2016) 463–493, https://doi.org/10.1111/odi.12446.

[8] W. Horton, S. Peerannawar, B. Török, M. Török, Theoretical and experimental analysis of the antioxidant features of substituted phenol and aniline model compounds, Struct. Chem. 30 (2018) 23–35, https://doi.org/10.1007/s11224-018-1183-4.

[9] M. Moalin, G. P. F. Van Strijdonck, M. Beckers, G. J. Hagemen, P. J. Borm, A. Bast, G. R. M. M. Haenen, A Planar Conformation and the Hydroxyl Groups in the B and C Rings Play a

Pivotal Role in the Antioxidant Capacity of Quercetin and Quercetin Derivatives, Molecules 16 (2011) 9636–9650, https://doi.org/10.3390/molecules16119636.

[10] C. Heijnen, G. Haenen, F. van Acker, W. van der Vijgh, A. Bast, Flavonoids as peroxynitrite scavengers: The role of the hydroxyl groups, Toxicol. Vitr. 15 (2001) 3–6, https://doi.org/10.1016/S0887-2333(00)00053-9.

[11] V.L. Singleton, R. Orthofer, R. M. Lamuela-Raventós, Analysis of total phenols and other oxidation substrates and antioxidants by means of folin-ciocalteu reagent, Meth. Enzymol. 299 (1999) 152–178, https://doi.org/10.1016/S0076-6879(99)99017-1.

[12] X. Li, Q. Jiang, T. Wang, J. Liu, D. Chen, Comparison of the Antioxidant Effects of Quercitrin and Isoquercitrin: Understanding the Role of the 6”-OH Group, Molecules 21 (2016) 1246, https://doi.org/10.3390/molecules21091246.

[13] C. Galanakis, Z. Tacer-Caba, The Concept of Superfoods in Diet. In The Role of Alternative and Innovative Food Ingredients and Products in Consumer Wellness, Academic Press: London 2020.

[14] G. Litwinienko, K. U. Ingold, Abnormal Solvent Effects on Hydrogen Atom Abstractions. 1. The Reactions of Phenols with 2,2-Diphenyl-1-picrylhydrazyl (dpph•) in Alcohols, J. Org. Chem. 68 (2003) 3433–3438, https://doi.org/10.1021/jo026917t.

[15] J. T. Banks, K. U. Ingold, J. Lusztyk, Measurement of Equilibrium Constants for Complex Formation between Phenol and Hydrogen-Bond Acceptors by Kinetic Laser Flash Photolysis, J. Am. Chem. Soc. 118 (1996) 6790–6791, https://doi.org/10.1021/ja961032i.

[16] M. Siah, M. Farzaei, H. Ashrafi-Kooshk Adibi, S. Arab, M. Rashidi, R. Khodarahmi, Inhibition of guinea pig aldehyde oxidase activity by different flavonoid compounds: an in vitro study, Bioorg. Chem. 64 (2016) 74–84, https://doi.org/10.1016/j.bioorg.2015.12.004.

[17] Z. Lu, G. Nie, P. S. Belton, H. Tang, B. Zhao, Structure–activity relationship analysis of antioxidant ability and neuroprotective effect of gallic acid derivatives, Neurochem. Int. 48 (2006) 263–274, https://doi.org/10.1016/j.neuint.2005.10.010.

[18] S. Jagan, G. Ramakrishnan, P. Anandakumar, S. Kamaraj, T. Devaki, Antiproliferative potential of gallic acid against diethylnitrosamine-induced rat hepatocellular carcinoma, Mol. Cell. Biochem. 319 (2008) 51–59, https://doi.org/10.1007/s11010-008-9876-4.

[19] S. Choubey, L. Varughese, V. Kumar, V. Beniwal, Medicinal importance of gallic acid and its ester derivatives: a patent review, Pharm. Pat. Anal. 4 (2015) 305–315, https://doi.org/10.4155/ppa.15.14.

[20] S. Mard, S. Mojadami, Y. Farbood, M. Gharib Naseri, The anti-inflammatory and anti-apoptotic effects of gallic acid against mucosal inflammation- and erosions-induced by gastric ischemia-reperfusion in rats, Vet. Res. Forum 6 (2015) 305–311.

[21] L. Socrier, A. Quéro, M. Verdu, Y. Song, R. Molinié, D. Mathiron, S. Pilard, F. Mesnard, S. Morandat, Flax phenolic compounds as inhibitors of lipid oxidation: elucidation of their mechanisms of action, Food Chem. 274 (2019) 651–658, https://doi.org/10.1016/j.foodchem.2018.08.126.

[22] L L. Fási, F. Di Meo, C.-Y. Kuo, S. Stojkovic Buric, A. Martins, N. Kúsz, Z. Béni, M. Dékány, G.T. Balogh, M. Pesic, Antioxidant-inspired drug discovery: antitumor metabolite is formed in situ from a hydroxycinnamic acid derivative upon free radical scavenging, J. Med. Chem. 62 (3) (2019) 1657–1668, https://doi.org/10.1021/acs.jmedchem.8b01994.

[23] G. I. Russo, D. Campisi, M. Di Mauro, F. Regis, G. Reale, M. Marranzano, R. Ragusa, T. Solinas, M. Madonia, S. Cimino, Dietary consumption of phenolic acids and prostate cancer: a case-control study in Sicily, Southern Italy, Molecules 22 (2017) 2159, https://doi.org/10.3390/molecules22122159.

[24] C. S. Yang, J. M. Landau, M. T. Huang, H. L. Newmark, Inhibition of carcinogenesis by dietary polyphenolic compounds, Ann. Rev. Nutr. 21 (2001) 381–406, https://doi.org/10.1146/annurev.nutr.21.1.381.

[25] I. T. Johnson, G. Williamson, S. R. R. Musk, Anticarcinogenic factors in plant foods: A new class of nutrients?, Nutr. Res. Rev. 7 (1994) 175–204, https://doi.org/10.1079/NRR19940011.

[26] A. García-Lafuente, E. Guillamón, A. Villares, M. A. Rostagno, J. A. Martínez, Flavonoids as antiinflammatory agents: implications in cancer and cardiovascular disease, Inflamm. Res. 58 (2009) 537–552, https://doi.org/10.1007/s00011-009-0037-3.

[27] M. Athar, J. H. Back, X. Tang, K. H. Kim, L. Kopelovich, D. R. Bickers, A. L. Kim, Resveratrol: a review of preclinical studies for human cancer prevention, Toxicol. Appl. Pharmacol. 224 (2007) 274–283, https://doi.org/10.1016/j.taap.2006.12.025.

[28] I. Boček, K. Starčević, I. Novak Jovanović, R. Vianello, M. Hranjec, Novel imidazo[4,5-*b*]pyridine derived acrylonitriles: A combined experimental and computational study of their antioxidative potential, J. Mol. Liq. 342 (2021) 117527, https://doi.org/10.1016/j.molliq.2021.117527.

[29] J. Ferlay, M. Colombet, I. Soerjomataram, C. Mathers, D. M. Parkin, M. Pineros, A. Znaor, F. Bray, Estimating the global cancer incidence and mortality in 2018: GLOBOCAN sources and methods, Int. J. Cancer 144 (2019) 1941–1953, https://doi.org/10.1002/ijc.31937.

[30] R. L. Siegel, K. D. Miller, A. Jemal, Cancer statistics, 2020, CA Cancer J. Clin. 70 (2020) 7–30, https://doi.org/10.3322/caac.21590.

[31] N. Durand, P. Storz, Targeting reactive oxygen species in development and progression of pancreatic cancer, Expert. Rev. Anticancer. Ther. 17(1) (2017) 19–31, https://doi.org/10.1080/14737140.2017.1261017.

[32] E. Vitaku, D. T. Smith, J. T. Njardarson, Analysis of the Structural Diversity, Substitution Patterns, and Frequency of Nitrogen Heterocycles among U.S. FDA Approved Pharmaceuticals, J. Med. Chem. 57 (2014) 10257–10274, https://doi.org/10.1021/jm501100b.

[33] D. Akwata, A. L. Kempen, J. Lamptey, N. Dayal, N. R. Brauer, H. O. Sintim, RSC Med. Chem. 15 (2024) 178–192, https://doi.org/10.1039/d3md00415e.

[34] G. Li Petri, C. Pecoraro, O. Randazzo, S. Zoppi, S. M. Cascioferro, B. Parrino, D. Carbone, B. El Hassouni, A. Cavazzoni, N. Zaffaroni, G. Cirrincione, P. Diana, G. J. Peters, E. Giovannetti, New Imidazo[2,1-*b*][1,3,4]Thiadiazole Derivatives Inhibit FAK Phosphorylation and Potentiate the Antiproliferative Effects of Gemcitabine Through Modulation of the Human Equilibrative Nucleoside Transporter-1 in Peritoneal Mesothelioma, Anticancer. Res. 40 (9) (2020) 4913–4919, https://doi.org/10.21873/anticanres.14494.

[35]S. Cascioferro, G. L. Petri, B. Parrino, D. Carbone, N. Funel, C. Bergonzini, G. Mantini, H. Dekker, D. Geerke, G. J. Peters, G. Cirrincione, E. Giovannetti, P. Diana, Imidazo[2,1-b][1,3,4]thiadiazoles with antiproliferative activity against primary and gemcitabine-resistant pancreatic cancer cells, Eur. J. Med. Chem. 189 (2020) 112088, https://doi.org/10.1016/j.ejmech.2020.112088.

[36] D. Carbone, M. De Franco, C. Pecoraro, D. Bassani, M. Pavan, Stella Cascioferro, B. Parrino, G. Cirrincione, S. Dall'Acqua , S. Moro, V. Gandin,P. Diana, Discovery of the 3-Amino-1,2,4-triazine-Based Library as Selective PDK1 Inhibitors with Therapeutic Potential in Highly Aggressive Pancreatic Ductal Adenocarcinoma, Int. J. Mol. Sci. 24 (2023) 3679, https://doi.org/10.3390/ijms24043679.

[37] A. Beč, L. Racane, L. Žonja, L. Persoons, D. Daelemans, K. Starčević, R. Vianello, M. Hranjec, Biological evaluation of novel amidino substituted coumarin-benzazole hybrids as promising therapeutic agents, RSC Med. Chem. 14 (2023) 957–968, https://doi.org/10.1039/D3MD00055A.

[38] M. Cindrić, I. Sović, M. Mioč, L. Hok, I. Boček, P. Roškarić, K. Butković, I. Martin-Kleiner, K. Starčević, R. Vianello, M. Kralj, M. Hranjec, Experimental and Computational Study of the Antioxidative Potential of Novel Nitro and Amino Substituted Benzimidazole/Benzothiazole-2-Carboxamides with Antiproliferative Activity**,** Antioxidants 8 (2019) 477, https://doi.org/10.3390/antiox8100477.

[39] G. Serdaroğlu, N. Uludağ, E. Ercag, P. Sugumar, P. Rajkumar, Carbazole derivatives: Synthesis, spectroscopic characterization, antioxidant activity, molecular docking study, and the quantum chemical calculations, J. Mol. Liq. 330 (2021) 115651, https://doi.org/10.1016/j.molliq.2021.115651.

[40] A. A. Altalhi, H. E. Hashem, N. A. Negm, E. A. Mohamed, E. M. Azmy, Synthesis, characterization, computational study, and screening of novel 1-phenyl-4-(2-phenylacetyl)-thiosemicarbazide derivatives for their antioxidant and antimicrobial activities, J. Mol. Liq. 33 (2021) 115977, https://doi.org/10.1016/j.molliq.2021.115977.

[41] M. Toma, L. Božičević, J. Lapić, S. Đaković, D. Šakić, T. Tandarić, R. Vianello, V. Vrček, Transacylation in Ferrocenoyl-Purines. NMR and Computational Study of the Isomerization Mechanism, J. Org. Chem. 84 (2019) 12471–12480, https://doi.org/10.1021/acs.joc.9b01944.

[42] A. Alizadeh, A. Bagherinejad, J. Kayanian, R. Vianello, An experimental and computational study of new spiro-barbituric acid pyrazoline scaffolds: restricted rotation vs. annular tautomerism, New. J. Chem. 46 (2022) 7242–7252, https://doi.org/10.1039/D1NJ06208E.

[43] E. Mehić, L. Hok, Q. Wang, I. Dokli, M. Svetec Miklenić, Z. Findrik Blažević, L. Tang, R. Vianello, M. Majerić Elenkov, Expanding the Scope of Enantioselective Halohydrin Dehalogenases – Group B, Adv. Synth. Catal. 364 (2022) 2576–2588, https://doi.org/10.1002/adsc.202200342.

[44] T. Tandarić, R. Vianello, Computational Insight into the Mechanism of the Irreversible Inhibition of Monoamine Oxidase Enzymes by the Antiparkinsonian Propargylamine Inhibitors Rasagiline and Selegiline, ACS Chem. Neurosci. 10 (2019) 3532–3542, https://doi.org/10.1021/acschemneuro.9b00147.

[45] Gaussian 16, Revision C.01, M. J. Frisch, G. W. Trucks, H. B. Schlegel, G. E. Scuseria, M. A. Robb, J. R. Cheeseman, G. Scalmani, V. Barone, G. A. Petersson, H. Nakatsuji, X. Li, M. Caricato, A. V. Marenich, J. Bloino, B. G. Janesko, R. Gomperts, B. Mennucci, H. P. Hratchian, J. V. Ortiz, A. F. Izmaylov, J. L. Sonnenberg, D. Williams-Young, F. Ding, F. Lipparini, F. Egidi, J. Goings, B. Peng, A. Petrone, T. Henderson, D. Ranasinghe, V. G.

Zakrzewski, J. Gao, N. Rega, G. Zheng, W. Liang, M. Hada, M. Ehara, K. Toyota, R. Fukuda, J. Hasegawa, M. Ishida, T. Nakajima, Y. Honda, O. Kitao, H. Nakai, T. Vreven, K. Throssell, J. A. Montgomery, Jr., J. E. Peralta, F. Ogliaro, M. J. Bearpark, J. J. Heyd, E. N. Brothers, K. N. Kudin, V. N. Staroverov, T. A. Keith, R. Kobayashi, J. Normand, K. Raghavachari, A. P. Rendell, J. C. Burant, S. S. Iyengar, J. Tomasi, M. Cossi, J. M. Millam, M. Klene, C. Adamo, R. Cammi, J. W. Ochterski, R. L. Martin, K. Morokuma, O. Farkas, J. B. Foresman, and D. J. Fox, Gaussian, Inc., Wallingford CT, 2016.

[46] D. Huang, B. Ou, R. L. Prior, The Chemistry behind Antioxidant Capacity Assays, J. Agric. Food Chem. 53 (2005) 1841–1856, https://doi.org/10.1021/jf030723c.

[47] C. Hu, G. You, J. Liu, S. Du, X. Zhao, S. Wu, Study on the mechanisms of the lubricating oil antioxidants: Experimental and molecular simulation, J. Mol. Liq. 324 (2021) 115099, https://doi.org/10.1016/j.molliq.2020.115099.

[48] A. Benayahoum, S. Bouakkaz, T. Bordjiba, M. Abdaoui, Antioxidant activity and pK_a calculations of 4-mercaptostilbene and some derivatives: A theoretical approach, J. Mol. Liq. 275 (2019) 221–231, https://doi.org/10.1016/j.molliq.2018.11.092.